Carbon Burial in the Mid-Latitude Fjords of Scotland

Craig Smeaton[1*], Handong Yang[2] and William E.N. Austin[1,3]

[1]School of Geography & Sustainable Development, Irvine Building, North Street, University of St Andrews, Fife, KY16 9AL, UK.

[2]Department of Geography, University College London, North-West Wing, Gower Street, London WC1E 6BT, UK

[3]Scottish Association of Marine Science, Scottish Marine Institute, Oban, Argyll, PA37 1QA

*Corresponding Author: Craig Smeaton (cs244@st-andrews.ac.uk)

Highlights

- 84,000 tonnes of OC is buried annually in the sediments of Scottish fjords.
- Annually, Scottish fjords bury as much OC as the North Sea.
- OC accumulates in Scottish fjords at a rate exceeding global averages for fjords.
- The OC that is buried in Scottish fjord sediments is largely marine in origin.
- Regional oceanography and geomorphology drive the OCARs in fjords.

Keywords

Fjords; sedimentation; radiometric dating; organic carbon; carbon storage; radiocarbon

Abstract

Fjord sediments are recognised global hotspots for the burial of organic carbon (OC) and as an integral part of the global carbon (C) cycle. Relative to their spatial extent, more OC is trapped and stored in the sediments of fjords than any other marine sedimentary environment. Until recently, our understanding of the rate at which OC accumulates and is buried in mid-latitude fjord sediments was poor, as these systems have largely been overlooked in favour of their high latitude counterparts. In this study, we quantify and explore the drivers of OC burial in the mid-latitude fjords of Scotland. By examining fifteen sediment cores from ten fjords, it is estimated that on average 57.1 ± 10.9 g C m^{-2} yr^{-1} accumulates in the sediments of Scottish fjords, exceeding observed OC burial in other vegetated fjord systems. When combined with an understanding of the spatial heterogeneity of the fjord sediments, it is estimated that Scottish fjords bury 84,000 tonnes of OC annually, which is equivalent to the whole North Sea sedimentary system, despite the area of the latter being approximately 190 times larger. These findings highlight that mid-latitude fjords play a more significant role in global carbon cycling than previously thought, providing highly effective burial and storage of OC in fjord sediments.

1. Introduction

Through the capture and burial of globally significant quantities of OC in their sediments (Cui et al., 2016; Smeaton et al., 2017; Smith et al., 2015) fjords play an important role in the coastal and wider marine C cycle (Bauer et al., 2013). Globally, it is estimated that fjord sediments bury 18 Mt OC yr^{-1}, accounting for approximately 11% of annual marine C burial globally (Cui et al., 2016; Smith et al., 2015). High-latitude fjords are characterised by steep catchments, shallow sills, relatively short transport times of OC from land to the sea and high sedimentation rates (Bianchi et al., 2020; Howe et al., 2010; Syvitski et al., 1987). These features enhance the capture of terrestrially derived OC (OC_{terr}) in high-latitude fjords, making them hotspots for OC burial (Cui et al., 2016; Smith et al., 2015). It is clear that fjords provide an important climate regulation service by capturing and storing OC that would potentially have been re-mineralized and returned to the atmosphere as CO_2, yet mid-latitude fjords have largely been overlooked in estimates of global OC burial because of the sparsity of available data. Mid-latitude fjords have many of the same characteristics as their high-latitude counterparts (Bianchi et al., 2020; Syvitski et al., 1987) but tend to be less restricted and more open to the adjacent continental shelf and the influence of the marine environment (Austin and Inall, 2002; Faust and Knies, 2019). These factors potentially allow different mechanisms to govern the burial and storage of OC between mid- and high-latitude fjords.

The fjords of Scotland provide an opportunity to better understand the role of mid-latitude fjords within the marine carbon cycle. The sediments within the fjords of Scotland have been shown to contain nationally significant OC stores, with an estimated 252 ± 62 Mt of OC held within their post-glacial sediments, which have been accumulating since the retreat of regional ice cover ~ 13,500 years ago (Bradwell et al., 2021; Clark et al., 2012; Smeaton et al., 2017, 2016). It is estimated that 42 ± 10% of the OC held within the surface sediments is terrestrial in origin (Smeaton and Austin, 2017), lower than the global average of 55 – 62% (Cui et al., 2016).

Additionally, Scottish fjords are the only fjord system in the world where the spatial heterogeneity of both sediment type and OC content at the seabed has been mapped (Smeaton et al., 2021b; Smeaton and Austin, 2019). Both measures are crucial but often overlooked when quantifying OC stocks and burial rates; even though differences in grain size and sediment type are known to strongly influence OC composition and the rate at which C accumulates on the seabed of fjords (Hage et al., 2020; Hunt et al., 2020; Prior et al., 1986; Włodarska - Kowalczuk et al., 2019). Until now, the largest unknown within Scottish fjords has been the rate at which OC accumulates and is incorporated into the long-term OC sedimentary stores.

In this study, we: (**i**) quantify OC burial across a number of Scottish fjords, (**ii**) estimate the amount of OC buried across all Scottish fjords annually, taking into consideration the spatial heterogeneity of the sediments, and (**iii**) determine the source of the OC. Through a better understanding of these factors, we aim to provide greater insight into the mechanisms which govern the modern deposition, burial and storage of OC in mid-latitude fjords. These insights allow comparisons to be made with high-latitude fjord systems and allow the role these mid-latitude fjords play in the marine C cycle to be better defined.

2. Methods & Materials

2.1 Study Sites

There are 226 fjords found across the west coast and the islands of Scotland, these can be characterised as 111 large fjords (over 2 km long, with fjord length twice fjord width) (Edwards and Sharples, 1986) and 115 smaller systems. Scotland's fjords are comparable to other temperate vegetated systems, such as those found in Norway, New Zealand, Chile and North America (Bianchi et al., 2020; Howe et al., 2010; Syvitski et al., 1987). As with fjords globally, their catchment and submarine geomorphology defines their ability to bury and store OC (Bianchi et al., 2020; Syvitski and Shaw, 1995). Previous studies have shown that Scotland's fjords can be characterised into several groups based on their glacial history and resultant geomorphology (Smeaton et al., 2017). The mainland and Inner Hebrides are classic fjords characterized by heavily glaciated geomorphology with over-deepened basins (Howe et al., 2002; Syvitski and Shaw, 1995), while the Outer Hebrides and the Shetland islands systems are shallower with a more subdued submarine geomorphology and could equally be referred to as fjards. Fjards are narrow and, like fjords, the products of glacial processes, but unlike classical fjords they are relatively shallow and flat-bottomed and lack the geomorphological characteristics key to the accumulating sediment at high rates (Syvitski et al., 1987). This geomorphological difference results in the mainland fjords being the main repositories for the 252 ± 62 Mt of OC stored in the postglacial sediments of Scotland's fjord network (Smeaton et al., 2017). This study will therefore focus on the mainland fjords from Loch Eriboll the most northerly fjord to the more southerly fjords within the Loch Linnhe complex (Fig.1).

2.3 Sampling

Fifteen sediment cores were collected from 10 mid-latitude fjords between 2016-2019 (Fig.1B-G). Multi-cores (~50 cm long) were collected from Loch Eriboll, Loch Gairloch, Loch Torridon and Loch Carron from on-board the *MRV Alba na Mara* in June 2018. Further, multi-cores where collected from Loch Eishort, Loch Nevis and Loch Hourn (Fig.1B-D) from the *MRV Scotia* in July 2019 (Fig.1 E-F). Sholkovitch cores (~50 cm long) were collected from Loch Sunart, Loch Creran and Loch Etive from on-board the *RV Seòl Mara* and *R.V. Calanus* throughout 2016 (Fig.1G). At each coring site the location and the water depth were recorded alongside the sediment type described using the Folk classification scheme (Folk, 1954) (*Supplementary Table 1*).

Once retrieved the cores were extruded and sliced at 1 cm intervals, any shells found within the sediment were set aside for potential radiocarbon (^{14}C) dating. The samples were weighed to determine wet bulk density values and frozen on-board the vessels before being returned to the University of St Andrews for analysis.

2.4 Bulk Elemental and Stable Isotope analysis

Each 1 cm slice was freeze dried and weighed allowing the calculation of water content and dry bulk density following the methodology of Dadey et al. (1992). Samples were taken at 2 cm intervals from each of the cores and homogenized to a fine powder. To determine the bulk elemental (OC and N) and stable isotope ($\delta^{13}C_{org}$ and $\delta^{15}N$) composition approximately 12 mg of processed sediment was placed into tin capsules and sealed; a further 12 mg was placed into silver capsules. The samples encapsulated in silver underwent acid fumigation (Harris et al., 2001) to remove carbonate ($CaCO_3$) and were dried for 24 hrs at 40°C. The stable isotope analyses were undertaken at OEA labs using an elemental analyser coupled to an isotope ratio mass spectrometer (EA-IRMS). The acidified samples were analysed for OC and $\delta^{13}C_{org}$, while nitrogen (N) and $\delta^{15}N$ values were produced from the tin encapsulated samples. By analysing the N and $\delta^{15}N$ separately, we negate the potential risk of altering these values through the acid fumigation step (Kennedy et al., 2005). Triplicate measurements of samples ($n = 25$) produced standard deviations (1σ) of 0.01 % for N and 0.06 ‰ for $\delta^{15}N$, 0.03 % for OC and 0.08 ‰ for $\delta^{13}C_{org}$. Further quality control was assured by repeat analysis of high OC sediment standard (B2151) with reference values for C of 7.45 ± 0.14 %, $\delta^{13}C$ of -28.85 ± 0.10 ‰, N of 0.52 ± 0.02 % and $\delta^{15}N$ of 4.32 ± 0.2. The reference standards ($n=30$) deviated from the known values by: OC = 0.07 %, $\delta^{13}C$ = 0.11 ‰, N = 0.02 % and $\delta^{15}N$ = 0.13 ‰. The isotope values are reported in standard delta notation relative to Vienna Peedee belemnite (VPDB) and air. The C/N and N/C ratios are reported as molar ratios: C/N = (OC/12)/(N/14); N/C = (N/14)/(OC/12).

2.5 Fraction of Terrestrial OC

To estimate the fraction of terrestrial (F_{terr}) and marine (F_{mar}) OC in the sediments, the $\delta^{13}C_{org}$, $\delta^{15}N$ and the N/C values were used in combination with a binary mixing model (Cui et al., 2016; Faust and Knies, 2019) as well as a Bayesian isotope mixing model (Smeaton and Austin, 2017). The N/C ratio was chosen over the more commonly used C/N ratio, as the N/C ratio represents changes in OC rather than N (Moossen et al., 2013; Perdue and Koprivnjak, 2007). The terrestrial ($\delta^{13}C_{org}$: -28. ± 0.9 ‰ ; $\delta^{15}N$: 1.3 ± 2.2 ‰ ; N/C: 0.04 ± 0.02) and marine ($\delta^{13}C_{org}$: -18.7 ± 2.1 ‰ ; $\delta^{15}N$: 5.3 ± 2.1 ‰ ; N/C: 0.10 ± 0.03) source values were obtained from Smeaton and Austin, (2017); these samples were collected from the catchments and foreshore of fjords on the west coast of Scotland (*Supplementary Table 2-3*). The terrestrial source values utilised in this study differ little from those used in other studies of temperate vegetated fjords (Cui et al., 2016; Faust and Knies, 2019; Hinjosa et al., 2014). In contrast, the marine N/C source values are lower than those observed in other fjord systems (Bertrand et al., 2012; Cui et al., 2016; Hinjosa et al., 2014), this difference is driven by the inclusion of macro-algae in the determination of the marine source value. The coastlines of Scotland's fjords are dominated by macro-algae that are potentially a significant source of OC to the sediments (Burrows et al., 2017, 2014) therefore we consider the inclusion of these samples in determining a representative marine source value for the region as a crucial step.

Metamorphic and igneous rocks dominate the catchments of the fjords in this study with sparse outcrops of sedimentary material. Recent studies indicate that there is minimal fossil/pyrogenic OC (< 0.1 % OC) input to the Scottish fjords (Smeaton et al., 2021a) therefore, it is likely OC derived from the bedrock geology will have a minimal impact on the bulk elemental and isotopic values. The degradation of the organic matter (OM) down-core may potentially influence the outputs from the models as the marine-derived OC (OC_{mar}) is more likely to be lost and OC_{terr} to be preferentially preserved (Arndt et al., 2013; Derrien et al., 2020; Larowe et al., 2020; Middelburg, 2018), therefore caution must be applied in down-core studies when interpreting the outputs from the end-member mixing models.

The binary (or two end-member) mixing model based upon Thornton and McManus, (1994) was employed to calculate the fraction of terrestrial OM in the sediment. $\delta^{13}C_{org}$ and N/C values were used as tracers independently from one another with the binary mixing model (*eq. 1-4*).

$$F_{terr} = \frac{(\delta^{13}C_{mar} - \delta^{13}C_{terr})}{(\delta^{13}C_{mar} - \delta^{13}C_{sample})} \qquad (eq.1)$$

$$F_{terr} = \frac{(N/C_{mar} - N/C_{terr})}{(N/C_{mar} - N/C_{sample})} \qquad (eq.2)$$

$$F_{terr} + F_{mar} = 1 \qquad (eq.3)$$

$$\%OC_{terr} = F_{terr} \times \%OC \qquad (eq.4)$$

The binary mixing model calculations were carried out in combination with Markov chain Monte Carlo (MCMC) simulations in the OpenBUGS software (Lunn et al., 2009). Simply, 100,000 out of 1,000,000 random samples from a normal distribution of each end-member were taken to populate the mixing model calculation steps (*eq. 1-4*), resulting in a significant number of solutions being generated for each sample. The mean, range and standard deviation of the F_{terr} were calculated for each sample from the MCM solutions.

The open source Bayesian isotope mixing model FRUITS (Fernandes et al., 2014) which uses multiple tracers ($\delta^{13}C_{org}$, $\delta^{15}N$, N/C) concurrently within a Bayesian framework was also utilised following the approach of Smeaton and Austin, (2017). This approach allows the estimation of the proportional contribution of terrestrial and marine derived OC and provides a direct comparison with the simpler binary models.

2.6 Grain Size Analysis

Grain size was measured using a Beckman Coulter LS230 laser particle size analyser. The lithic fraction of the material was isolated by boiling the samples in hydrogen peroxide (H_2O_2) and 10 % hydrochloric acid (HCl) to remove OM and $CaCO_3$. Prior to analysis 5 % sodium hexametaphosphate solution was add to the sample to assure full disaggregation of the particles. The quantity of sample introduced to the analyser was varied to obtain a laser beam obscuration between 8% and 12%. No sample contained particles >2000 μm. From the grain size data the simplified folk classification was derived (Kaskela et al., 2019).

2.7 Radiometric Dating

Lead-210 (half-life of 22.3 year) is a naturally-produced radionuclide, derived from atmospheric fallout described as unsupported or excess ($^{210}Pb_{ex}$). Cesium-137 (half-life of 30 years) and Americium-241 (half-life of 432.2 years) are artificially produced radionuclides, introduced to the study area by atmospheric fallout from nuclear weapons testing and nuclear reactor release. These tracers have been extensively used in the dating of recent sediments, providing chronological control on the last 100-150 years (Robbins, 1978).

After freeze drying, the samples were weighed to determine sample specific dry bulk density and porosity values (Appleby et al., 1986). Fifteen fjord cores were analysed for ^{210}Pb, ^{226}Ra,

^{137}Cs by direct gamma assay jointly between the Environmental Radiometric Facility at University College London and the Scottish Association of Marine Sciences (SAMS). The analyses were carried out using ORTEC HPGe GWL series well-type coaxial low background intrinsic germanium detector. Lead-210 was determined via its gamma emissions at 46.5keV, and ^{226}Ra by the 295keV and 352keV gamma rays emitted by its daughter isotope ^{214}Pb following 3 weeks storage in sealed containers to allow radioactive equilibration. Cesium-137 and ^{241}Am were measured by their emissions at 662keV and 59.5keV respectively (Appleby et al., 1986). Americium-241 was measured only on the cores analysed at UCL. The absolute efficiencies of the detectors were determined using calibrated sources and sediment samples of known activity. Corrections were made for the effect of self-absorption of low energy gamma rays within the sample (Appleby and Oldfield, 1992).

Radiocarbon ages were acquired from shells (paired bivalves) found in six of the sediment cores; these were augmented by a further eight shells collected from sediment cores collected from other mainland fjords and the fjards of Shetland (*Supplementary Fig.1*). The radiocarbon was measured by accelerator mass spectrometer (AMS) at the ^{14}CHRONO Centre at Queens University Belfast. The radiocarbon dating was used to determine basal ages of each of the sediment cores. The radiocarbon dates were calibrated using OxCal 4.4 age modelling software (Ramsey and Lee, 2013), applying the Marine20 curve (Heaton et al., 2020; Reimer et al., 2020) and the regional marine radiocarbon reservoir age correction: ΔR value of -26 ± 14 yr (Cage et al., 2006).

2.8 Sediment and Carbon Accumulation

The ^{210}Pb and ^{137}Cs data have been used to calculate the linear sedimentation rates (LSR), mass accumulation rates (MAR) and organic carbon accumulation rates (OCAR). The simplest and most commonly used approach used in fjords to estimate depositional rates utilises the $^{210}Pb_{ex}$

($^{210}Pb_{total}$ – $^{210}Pb_{supported}$) data in conjunction with the constant flux–constant sedimentation (CF–CS) model (Krishnaswamy et al., 1971), to calculate LSRs. Using the CF-CS model LSRs were calculated for those cores which could be fitted with a logarithmic regression with $R^2 > 0.75$ (Ramirez et al., 2016). The ^{210}Pb derived LSRs are further constrained by LSRs calculated using ^{137}Cs. The peak of ^{137}Cs in the cores is attributed to fallout derived from nuclear weapons testing (peak - 1964) and the 1986 Chernobyl accident; these chronological markers allow LSRs to be calculated for the most recent intervals of the cores. MARs (g m^{-2} y^{-1}) were calculated by multiplying the LSR by core specific sediment bulk density values (*Supplementary Data*). The OCARs (gOC m^{-2} yr^{-1}) were calculated by multiplying the weight fraction of OC, which for each core is represented as the average % OC values of all 1 cm sediment slices (Smith et al., 2015). Similarly, the terrestrial OC accumulation rates ($OC_{terr}AR$) were calculated by multiplying the MAR by the average weight fraction of OC_{terr} determined by the isotope mixing models. Analytical uncertainties were propagated through all calculations and are given for each quantity. The approach produces globally comparable mean rates but there are inherent biases that must be recognized. The calculations are based on LSR, average OC and OC_{terr} values; this approach struggles to take into consideration changes in sedimentation, OC input and preservation conditions potentially leading to over- and under-estimations of the long-term rates. To overcome some of these issues, a burial efficiency correction can be used (Koziorowska et al., 2018; Sepulveda et al., 2011; Smith et al., 2015). The OC burial efficiency (%) for each core was calculated using the approach of Koziorowska et al. (2018). Simply, the OC concentration in the ~ 100 year old sediment layer was compared to the surficial sediments (*Supplementary Table. 8*) to determine the loss of OC due to degradation (Arndt et al., 2013; Larowe et al., 2020; Middelburg, 2018), this approach makes two assumptions: (**i**) after 100 years the OC is no longer undergoing quantitative alteration (**ii**) the input and source of the OC has not changed over this 100 year period. The burial efficiency for each core was applied to the OCAR to quantify the OC that is being buried annually (Smith et al., 2015). This approach allows comparison of both depositional and burial rates from other fjord systems (Cui et al., 2016; Duffield et al., 2017; Koziorowska et al., 2018; Ramirez et al., 2016; Smith et al., 2015).

The second approach utilises more complex ^{210}Pb dating models (Arias-Ortiz et al., 2018). There are several dating models that can be used to interpret $^{210}Pb_{ex}$ depth distributions in marine sediment with increasing complexity. The two models most commonly used are the constant rate of supply (CRS) model (Appleby and Oldfield, 1978) and the constant initial concentration (CIC) model (Robbins, 1978). For this study, the CRS model was selected over the CIC models because the non-monotonic variation in unsupported ^{210}Pb activities found in the sediment cores preclude their use.

The CRS model is based upon the assumption that there is a constant rate of supply of unsupported ^{210}Pb to the sediment (Appleby and Oldfield, 1978). The model assumes a constant flux of ^{210}Pb to the sediments through time. The initial specific activity is variable and inversely related to MAR with higher MAR leading to lower $^{210}Pb_{ex}$ and vice versa. The dating is based upon the comparison of $^{210}Pb_{ex}$ inventories below a given depth and the integration of $^{210}Pb_{ex}$ specific activity as a function of the cumulative mass with the overall $^{210}Pb_{ex}$ inventory in the sediment core (Appleby, 2002; Arias-Ortiz et al., 2018; Sanchez-Cabeza and Ruiz-Fernández, 2012). Again, the ^{137}Cs data can be used to check the quality of the CRS model by comparing the depth at which ^{137}Cs peaks of known age fit to the modelled age of that depth horizon. The MARs calculated using the CRS model were combined with depth-specific OC and OC_{terr} values to calculate the OCAR and $OC_{terr}AR$ through time. This approach to calculating OCARs and $OC_{terr}AR$ overcome many of the issue of the simpler linear approach, yet care must be taken when interpreting between changes in OC_{terr} and OC_{mar} input versus degradation effects (i.e. preferential degradation of OC_{mar}) (Arndt et al., 2013; Larowe et al., 2020; Middelburg, 2018).

The basal radiocarbon dates from the six cores also allow LSRs to be estimated. LSR's were calculated between the depth of shell in the sediment core and the core top, assuming a contemporary surface. We recognise that the calculations are crude and do not take into consideration factors such as compaction (Bird et al., 2004) and possible changes in sedimentation rate through time. Yet, these calculations provide initial insight into the long-term (100's to 1000's of years) LSR's of these fjord sediments allowing comparisons with modern depositional rates (^{210}Pb, ^{137}Cs).

3. Results & Discussion

3.1 Organic Carbon Content of Mid-Latitude Fjord Sediments

The OC content of the sediments vary both spatially and temporally across the studied fjords (Fig.2). The surface sediments at the coring sites have OC contents ranging between 0.8 and 6.2 % which is consistent with known OC values of surficial sediments from Scotland's fjords (Smeaton and Austin, 2017; Smeaton and Austin, 2019). The highest OC contents of the surficial sediments are found in cores from the upper basin of Loch Etive (Fig.1G) which is highly restricted (Howe et al., 2002; Nørgaard-pedersen et al., 2006) which enhances the fjord's ability to trap terrestrial OC, a feature which is reflected in the depleted $\delta^{13}C_{org}$ values (-27.7 ‰) found at these sites (Fig.2). Additionally, the restricted nature of the upper basin of Loch Etive results in long-term hypoxic conditions (Friedrich et al., 2014) which reduces OC degradation (Arndt et al., 2013; Larowe et al., 2020; Middelburg, 2018) explaining the high OC content observed in this fjord. The lowest OC content is observed in core MC-50 from the outer basin of Loch Gairloch (Fig.1C). Unlike Loch Etive this fjord is not restricted and is dominated by an open exchange with the adjacent marine environment, as illustrated by the enriched $\delta^{13}C_{org}$ values (-22.6 ‰) in the surficial layers of the core (Fig.2).

Marked differences between the cores from the upper basin of Loch Etive and the outer basin of Loch Gairloch are highlighted by sediment type (Table.1). The cores from Loch Etive are characterised with mean grain sizes ranging between 27.6-36.1 µm with >80 % of the material being < 63 µm. Core GC-50 has a mean grain size 62.9 ± 12.6 µm but <50% of the grains are <63 µm. When characterised using the simplified Folk scheme (Kaskela et al., 2019) the cores from Loch Etive are characterised as mud to muddy sand while GC-50 is a mixed sediment. Finer grained and in-turn higher surface area sediments are generally associated with of high OC contents (Hunt et al., 2020; Keil et al., 1997; Mayer, 1994; McBreen et al., 2008), the different types of sediment within Loch Etive and Gairloch are therefore likely to be a major determinant in the difference in OC content observed. From the fifteen cores examined as part of this study, all with exception of GC-50, classified as mud to muddy sand (Table.1).

Stratigraphically, the OC content is highly changeable down core at almost all sites. The simplest explanation for this is the degradation of the OM, classical degradation curves can be observed in cores SM-16-2, SM(2)-16-3 and Cal-16-22, where the OC content decreases down core (Fig.2). Yet the $\delta^{13}C_{org}$ profiles do not support this simplistic view, because degradation alone would likely result in the preferential preservation of the more recalcitrant terrestrial over the highly labile marine OM (Blair and Aller, 2012; Keil et al., 1997) (Fig.2). In such cases, $\delta^{13}C_{org}$ values should be depleted down core in comparison to the core tops; this is not the case in the majority of the cores, which suggests more complex mechanisms governing the supply and burial of OC in these sediments.

When examined, the $\delta^{13}C_{org}$ profiles commonly follow the pattern of enriched values at the base and depleted values at the top of the core (Fig.2), which is the opposite of what is expected in profiles governed by OM degradation alone. These patterns are clearest in cores SM-16-2 (Loch Creran), Cal-16-22 (Loch Etive) and MC-74 (Loch Carron). Depleted $\delta^{13}C_{org}$ values are observed in the upper sections of all three cores in comparison to the $\delta^{13}C_{org}$ values found at depth, the most likely explanation for this is increased terrestrial OC input to the fjord sediments in recent times. The catchments of Scotland's fjords have undergone significant changes over time, with a move away from small scale subsistence farming to large scale sheep farming, the loss of natural woodland cover and the introduction of industrial forestry (Smout, 2004, 2003; Tipping, 2014). Such changes to the catchment have been shown to destabilise the catchment soils, resulting in an increased input of terrestrial OC to the fjords (Smeaton et al., 2021a); such changes are also likely to have caused the depleted $\delta^{13}C_{org}$ values found in the upper sections of the cores from these fjords (Fig.2). Of the many possible drivers of catchment destabilisation in the region in recent times (last 100 years), the widespread introduction of industrial forestry is the most likely (Moffat, 1988). However, the $\delta^{13}C_{org}$ profile of SM-16-2 displays the most extreme switch from enriched values of -22‰ to depleted values of -26‰ in the upper most section of the core. Core SM-16-2 is located in the outer basin of Loch Creran and it is unlikely that increased OC_{terr} alone could fully account for this significant shift in $\delta^{13}C_{org}$ values (Fig.2). The outer basin of Loch Creran does support several aquaculture sites and while core SM-16-2 is not located in the immediate vicinity of the aquaculture infrastructure itself, the core is down-fjord from an active aquaculture site. Over the last two decades the percentage of terrestrial OM in aquaculture feed has gradually increased to ~ 70 % (Shepherd et al., 2017); large inputs of this feed and associated faecal waste from the aquaculture is likely to be the main driver for the extreme shift towards the depleted $\delta^{13}C_{org}$ values at this site.

A few of the cores diverge from this pattern, core MC-70 (Loch Torridon) exhibits enriched $\delta^{13}C_{org}$ values with a lower OC content in the upper sections of the core in comparison to the lower OC content and depleted $\delta^{13}C_{org}$ values at depth with a marked change occurring at 30 cm (Fig.2). The core is located in the inner basin of Loch Torridon and it is unlikely that there has been a significant increase in marine OC input in recent times; furthermore, the reduction in OC content also favours a decrease in terrestrial input over an increase in marine input. The potential mechanisms that could drive such a shift are a significant reduction in terrestrial input which would normally be caused by extreme alterations to the catchment such as damming of the watercourse (Bianchi et al., 2015; Li et al., 2014), yet no such modification has occurred in the catchment of Loch Torridon. The more likely cause for the recent reduction in OC_{terr} supply is the catchment recovering from a past disturbance such as the loss of the natural woodland (Smout, 2004; 2003); the observed changes in OC and $\delta^{13}C_{org}$ profiles may therefore potentially reflect the return to pre-disturbance conditions of Loch Torridon.

The variability in the down core OC and $\delta^{13}C_{org}$ across the mid-latitude fjords illustrates that the quantity and source of the OC being trapped in the sediments has changed over time, with the upper sections of many cores being influenced by increasing terrestrial input from anthropogenic alterations of fjord catchments.

3.2 Quantifying Terrestrial and Marine Input

The $\delta^{13}C_{org}$, $\delta^{15}N$ and N/C values from the sediments collected from the 15 cores reveals a clear mixing line between marine and terrestrial OC (Fig.3) which is consistent with previous studies from Scottish fjords (Smeaton and Austin, 2017) and similar to other vegetated fjords around the world (Cui et al., 2016; Faust and Knies, 2019; Hinjosa et al., 2014). Using the bulk elemental and isotopic data in combination with the end-member mixing models, the fraction of terrestrial and marine OC within the sediment were determined. The outputs from the $\delta^{13}C_{org}$ binary end-member mixing model compare well to the Bayesian model output (R^2: 0.92) providing confidence in the estimates of the fraction of OC_{terr} (*Supplementary Fig.2*). In contrast the outputs from the N/C binary mixing model correlate poorly with both the $\delta^{13}C_{org}$ ($R^2 = 0.63$) and Bayesian mixing ($R^2 = 0.57$) model outputs, this is likely a consequence of the variability N/C values for the different OC sources (*Supplementary Table 2-3*). For the purposes of this study, the outputs from the Bayesian mixing model will be utilised as the outputs strongly correlate with the $\delta^{13}C_{org}$ binary mixing model, which provides confidence in the robustness of the results. Additionally, the model utilises the full range of terrestrial and marine source values and the outputs are therefore comparable to other temperate fjord systems.

Between 24 – 44 % of the OC at the coring sites originates from terrestrial sources. This supports previous estimates from Scotland that calculated that 42.0 ± 10.1 % of the OC stored in the surficial sediments of Loch Sunart and Tecuis was terrestrial in origin (Smeaton and Austin, 2017). Compared to other temperate fjords, these totals from Scotland are low as it is estimated that 55 – 62 % of the OC stored within the sediments of these fjords originates from the terrestrial environment (Cui et al., 2016). The relatively low OC_{terr} concentrations found within the sediments of these Scottish fjords in comparison to other temperate vegetated systems (table 3) is potentially due to a number of factors. The high OC_{terr} values in the fjords of New Zealand and Patagonia (Table 3) are potentially driven by differences in catchment vegetation with these Southern hemisphere fjords. The modern fjord catchments of New Zealand and Patagonia are often characterised by high vegetation densities (Avitabile et al., 2016, 2014) while Scotland's fjord catchments are today dominated by montane environments and low in biomass (Santoro et al., 2015), consequently reducing potential OC_{terr} input.

The openness and lack of restriction of exchange with the adjacent shelf (Edwards and Sharples, 1986) is another potential driver of the difference in OC_{terr} observed between the Scottish fjords and other systems. New Zealand fjords are highly restricted (Ramirez et al., 2016; Smith et al., 2015), often resulting in hypoxic and anoxic bottom waters which receive and preserve large quantities of OC_{terr}. In comparison, the Scottish fjords are well ventilated with regular flushing events (Austin and Inall, 2002; Gillibrand et al., 2005; Gillibrand and Amundrud, 2007) resulting in well oxygenated bottom waters and the sustained input of marine derived OC. Norwegian fjords have similar oceanographic conditions to their Scottish counterparts (Bianchi et al., 2020; Howe et al., 2010) and recent work has observed that the OC held in the sediments of some mainland Norwegian fjords is largely derived from marine sources (Faust and Knies, 2019). These findings suggest, rather than Scottish and Norwegian systems being outliers, that these more open well-ventilated fjords have been underrepresented in previous global compilations of fjord sediment data (Cui et al., 2016; Smith et al., 2015), in turn potentially overestimating the quantity of OC_{terr} held within fjords globally. Supplementary fig. 3 presents the down core profiles of OC_{terr} and OC_{mar}.

3.5 Linear Sedimentation and Mass Accumulation Rates

The radiometric dating of the sediments (*Supplementary Fig. 5-19, Supplementary Table 4*) allowed the LSRs and MARs to be calculated from three independent datasets (^{210}Pb, ^{137}Cs and ^{14}C). Estimations of LSRs and MARs derived from ^{14}C ages on marine shells are generally lower than those produced from the ^{210}Pb and ^{137}Cs data, which are measures of bulk sediment. The ^{14}C derived rates are based on basal ages (ranging between 47 – 3,065 years BP) from the cores analysed (*Supplementary Table 4*), this is likely to be the major source of the inconsistencies. Radiocarbon based age-control is used to estimate longer-term (100's to 1000's of years) sedimentation and accumulation rates which are impacted by sediment compaction (Bird et al., 2004) and alteration of the OM (Arndt et al., 2013; Larowe et al., 2020; Middelburg, 2018). In contrast, the similarity of the ^{210}Pb and ^{137}Cs based rates are explained as estimates of the modern deposition of material over similar time periods.

In addition, when MARs calculated using radiometric approaches are compared to sediment trap data, significant differences are observed. MARs determined using sediment trap data from Scottish fjords estimate rates of between 65.7 – 17,702 g m^{-2} yr^{-1} (Loh et al., 2010; Overnell and Young, 1995; Young, 1996). These sediments trap derived rates range from an order magnitude below to an order of magnitude above the sediment core-based estimates from this study. While sediment trap studies report data as LSRs and MARs they differ from radiometric measurements because these traps measure material falling through the water column and do not account for losses during transport, burial, compaction and remineralization of OM on the sea floor. The inconsistencies between dating methods mean that it is common when estimating LSRs and MSRs to attribute these differences to first-order remineralization and compaction of the OM (Baskaran et al., 2017). Baskaran et al. (2017) found that short-lived radioisotopes (^{210}Pb and ^{137}Cs) are more suited to determining modern depositional rates than radiocarbon and recommend where possible that the short-lived isotopes to be preferentially utilised in determining modern LSRs and MARs; our results (Fig.4) are consistent with their recommendations.

Across the 15 cores studied, the CF-CS based LSRs calculated using ^{210}Pb and ^{137}Cs range between 0.11 – 0.35 cm yr^{-1} and 0.13 - 0.26 cm yr^{-1} respectively. These LSRs are slightly lower overall than those reported in the very limited data from Scottish fjords but are at the lower boundary of LSR ranges observed in the temperate fjords of Chile, Norway and New Zealand (Table 2). The MARs derived from ^{210}Pb data range between 494 – 5,224 g m^{-2} yr^{-1} which compare well with other Scottish and temperate fjord data (Table 2). Neither LSRs nor MARs are observed to be linked to water column depth or distance from the head of the fjord (Fig.4). Instead, these rates are much more likely to be governed by submarine geomorphology, OM input and local oceanography (Ramirez et al., 2016). Full compilation of LSR and MAR data can be found in supplementary table 5-7.

The CRS dating models for each of the cores (*Supplementary Fig. 20-34*) provide greater insight into changes in LSRs and MARs through time than those calculated using the CF-CS model. The observed LSRs and MARs calculated using the CRS model for all cores fluctuate but in general, there is an upward trend in both LSRs and MARs in all but two of the cores (Cal-16-36, Cal-16-33). While many of these cores generally show this upward trend, the magnitude and timing of the increase in LSRs and MARs varies from site to site. Abrupt changes to sediment supply are common in the upper 5-10cm of the cores. These recent changes are likely driven by anthropogenic alteration of the catchments, in turn increasing the supply of sediment and potentially OC_{terr}. Cores Cal-16-36 and Cal-16-33 don't exhibit this upward trend in increasing depositional rates, but rather the LSR and MAR fluctuates throughout the core. Both cores are from the inner basin of Loch Etive, where it is highly likely that the changeability observed in the rates is governed by sediment supply from the terrestrial environment. The catchment of the inner basin of Loch Etive is unique among the study sites as the predominant land cover is blanket peat (Rannoch Moor). Peatlands are significantly more sensitive to changes in the environment (hydrology, temperature, etc.) than the other fjord catchments which are dominated by upland/montane land covers (Bragg and Tallis, 2001; Leifeld et al., 2012).

3.6 OC Accumulation Rates

The CF-CS based OCARs across the 15 cores studied vary between 35.5 – 110.9 g C m^{-2} yr^{-1}, with the greatest OCAR observed in the inner basin of Loch Torridon (Fig. 5A). The OCARs found in these mid-latitude fjords are consistently higher than those observed in other temperate fjord systems (Table 3), potentially suggesting a different mechanism governing the capture and burial of OC in these mid-latitude fjords. The OC_{terr} data suggest that the coring sites are heavily influenced by the marine environment with only 24 – 44 % of the OC originating from terrestrial sources (Table. 3), which is reflected by OC_{terr}ARs that tend to fall below global average values (Fig. 5B). Other studies (Hayes, 2001) report that the OC in Loch Duich's sediments were 84% terrestrial, but the coastal water exchange within this loch is extremely restricted and likely results in the high OC_{terr} content of the sediments. Recent work in Norwegian fjords has recorded that the OC held in the sediments is largely derived from marine sources and the OCARs here are higher than the global average (Faust and Knies, 2019). Faust and Knies (2019) determined that one of the likely drivers of these high OCARs was the strength of the North Atlantic Current (NAC), which provides the conditions (nutrients, salinity, temperature) to allow marine organisms to thrive and drive high OC_{mar} input. These findings further support and strengthen the evidence that the above global average OCARs observed in Scotland's fjords are due to the high OC_{mar} input likely due to regional oceanography, similar to that observed in Norwegian fjords (Faust and Knies, 2019) potentially. The fjords of Scotland are heavily influenced by the NAC and the Scottish Coastal Current (SCC) (Simpson and Hill, 1986); the SCC prevailing oceanographic current in the region which flows from the south between Scotland and Ireland (Fig.1A). The SCC and NAC are known transport pathways for nutrients (Heath et al., 2002; Pelegrí et al., 2006) which enhances coastal and near-shore primary productivity in the region (Holt et al., 2016). The supply of OC_{mar} to the fjord sediments is further enhanced by significant *in-situ* primary productivity (Johnston et al., 1977; Steele and Baird, 1962; Wood et al., 1973) driven by sheltered the low energy (Davies, 1975) conditions coupled to elevated nutrient input from both the marine and terrestrial environments (Gillibrand et al., 1996; Glud et al., 2016; Watts et al., 1998). The high primary productivity driven by local and regional oceanography observed around the west and northern coasts of Scotland (Holt et al., 2016) facilitates significant OC_{mar} input to the fjord sediments driving the high OCARs.

The OCARs and OC_{terr}AR calculated using the CF-CS approach provide a broad understanding of OC accumulation in these environments which are comparable to other fjord systems, but the method does not fully account for changes in OC input through time. The integration of the CRS dating models (*Supplementary Fig. 20-34*) with the OC and OC_{terr} data for each core provides a better understanding of potential temporal changes and drivers in OC accumulation.

Down core OCARs are either stable or decrease (Fig.6). This could be due to the *in situ* degradation of OC, or more likely changes in sediment and OC supply (Fig.2). The OC_{terr}ARs remain stable in the majority of cores, suggesting that changes in the marine environment govern the overall OC accumulation in the majority of the Scottish fjords. Exceptions do occur, for example in cores from the inner basin of Loch Creran and Loch Etive where increases in OC_{terr}AR mirror that of OCAR, suggesting that OC_{terr} plays a larger role in OC accumulation in these more restricted fjords (Fig.6). These findings further support the suggestion that the above average OCARs observed in the mid-latitude fjords of Scotland are a consequence of less restricted geomorphological settings, which facilitate improved circulation and enhanced OC_{mar} input.

3.7 OC Burial

Following the methodology of Koziorowska et al. (2018), the burial efficiency of OC was calculated for all cores (*Supplementary Table 8*). The burial efficiency is highly variable between sites, ranging between 35 – 98 %. The mean burial efficiency for the Scottish fjords was calculated as 77 ± 20 % which is in general agreement with the 80% burial efficiency utilised by Smith et al. (2015) in New Zealand fjords, but higher than the 63% burial efficiency observed in the Chilean fjords (Sepulveda et al., 2005). There are a significant number of mechanisms that govern the preservation of OC in sediments, the most common being the lability of the OM, bottom water oxygen concentration and sediment type (Arndt et al., 2013; Larowe et al., 2020; Middelburg, 2019). Beyond these more complex drivers could also be at play, such as armouring of the OM (Hemingway et al., 2019) and enhanced OM preservation promoted by iron (Lalonde et al., 2012). Therefore, to pin down the exact mechanism driving the burial efficiency is difficult. Further, the methodology of Koziorowska et al. (2018) assumes that OC input is consistent and does not change with time, but it is clear from the down core analyses of this study that OC inputs can change over time (Fig. 2). Therefore, while burial efficiencies are useful for making broad estimates of OC burial, caution must be applied when calculating and utilising this metric in fjords and systems where sediment supplies can rapidly change through anthropogenic or natural means.

Following the approach of Smith et al. (2015) which assumes each core is representative of an entire fjord; the OCARs (Table 3) are multiplied by the total area of the fjord allowing the total quantity of OC buried in each of the fjords to be estimated (Table 4). The 11 fjords (total area) within this study bury 21,621 ± 2,776 tonnes OC yr^{-1}. For comparison, Ramirez et al. (2016) calculated that all the fjords (total area) of New Zealand bury 35,773 tonnes OC yr^{-1}. However, this generic approach to estimating OC burial in sedimentary systems fails to take into consideration the heterogeneity of most sediments in coastal environments. The approach based on Smith et al. (2015) assumes the seabed is homogenous, predominantly consisting of muddy sediments because this is the sediment type where cores are normally recovered. Unlike many other fjord systems, the spatial heterogeneity of Scottish fjord sediments is increasingly well understood (Hunt et al., 2020; Smeaton et al., 2021b; Smeaton and Austin, 2019). It is estimated that only 39 % of the sediments in Scottish fjords are muddy (Smeaton et al., 2021b; Smeaton and Austin, 2019) and consequently, the OC burial estimates produced using the methodology of Smith et al. (2015) are likely an over estimation. By applying a fjord specific correction to account for heterogeneity of the seabed (*Supplementary Fig. 36-37*) we estimate that the muddy sediments held within the 11 fjords of this study bury 7,971 ± 1,139 tonnes OC yr^{-1}.

By applying the mean OCAR (58.62 ± 21.21 gC m^{-2} yr^{-1}) and burial efficiency (77 %) calculated from the 10 fjords in this study to all Scotland's 111 major fjords (2,608 km^2) it is estimated that they bury 0.118 ± 0.043 Mt OC yr^{-1} but, as noted above, this is likely to be an overestimation. Of the 15 cores collected as part of this study, 14 are from sediments classed as mud to muddy Sand and one (MC-51, Loch Gairloch) is classed as mixed sediment (Table 1) according to the simplified Folk classification (Folk, 1954; Kaskela et al., 2019). By applying the mean OCAR and burial efficiency to the areal extent of the different sediment types held within the fjords of Scotland (Table 5), we estimate that 0.046 Mt OC yr^{-1} and 0.038 Mt OC yr^{-1} are buried in the muddy and mixed sediments, respectively (Table 5). These two sediment types represent an estimated 67 % of the seabed of Scotland's fjords, while an additional 8.5 % of the seabed is classified as rock and incapable of burying OC (Smeaton and Austin, 2019, Smeaton et al., 2021). Therefore, we estimate that 75% of the sediments held within Scottish fjords bury an estimated 0.084 Mt OC yr^{-1}. The remaining 25% of sediments, which we do not have burial data for, are classified as coarse sediments and sand; these sediment types generally contain significantly less OC (Hunt et al., 2020; Keil and Mayer, 2014; McBreen et al., 2008; Smeaton et al., 2021b). Though recently, a number of studies of river dominated sedimentary systems have shown that rapidly deposited sands can retain large quantities of OC largely through the capture and storage of woody material (Lee et al., 2019; Sparkes et al., 2015). Within river dominated fjords (eg. Bute Inlet, Canada), turbidity currents have been observed to be important transport mechanism governing the storage and burial of OC in sands (Hage et al., 2020). However, the small river systems of the fjords of Scotland (Edwards and Sharples, 1986) are unlikely to contribute enough woody material to allow sands to be a major store of OC as reported by Hage et al., (2020). Available sediment measurements indicate that the coarser sediments of the mid-latitude fjords of Scotland will likely have low OCARs and low burial efficiencies; but they do occupy a significant seabed area of approximately 647 km^2 and will consequently play an additional but currently unquantified role in trapping and storing OC.

When compared to other regional marine sedimentary systems such as the North Sea (~500,000 km^2) which buries an estimated 0.1 Mt OC yr^{-1} (Haas et al., 1997), it is clear that the sediments with Scotland's mid-latitude fjords (~2,608 km^2) are of national and global importance.

4. Conclusion

Here we, investigated the variability of sediment and OC accumulation across the seabed of a number of fjords allowing the total annual OC burial within the sediments of all Scottish fjords to be estimated at 84,000 tonnes of OC. Across fifteen cores LSR's range between 0.11 – 0.35 cm yr^{-1} while MAR's values between 494 – 5,224 g m^{-2} yr^{-1} were observed. These rates compare favourably to those found in other temperate vegetated fjord systems globally. In contrast, we observe OCAR's of between 35.5 – 110.9 g C m^{-2} yr^{-1} which are above the global average, these heightened rates are primarily driven by OC_{mar} input with OC_{terr} only representing 22 – 44 % of the total OC found in the sediments of these fjords.

Current thinking suggests that fjords are hotspots of OC burial because of their highly restricted geomorphology, which induces low bottom water oxygenation and the enhanced capture of significant quantities of OC_{terr}. While it is likely that the quantity of OC_{terr} entering mid-latitude fjord sediments has increased in recent decades due to anthropogenic disturbance of the neighbouring terrestrial environment, the dominant competent of the OC stored within these sediments remains marine in origin. Above average OCARs found in these fjords are likely a product of high OC_{mar} input, which is likely governed by the strength of regional oceanographic currents similar to that observed in Norwegian fjords (Faust and Knies, 2019).

While the mechanisms, which govern the burial and storage of OC in the mid-latitude fjords of Scotland, may differ from their high-latitude counterparts, they nevertheless play an equivalent role in climate regulation through the burial and storage of OC within their sediments. We conclude that all fjord systems appear to stand-out in their capacity to bury globally significant quantities of OC in marine sediments.

Data Availability

All data produced as part of this research is included in the manuscript and supplementary material.

Acknowledgments

This project was supported by funding from the Scottish Blue Carbon Forum and BBSRC/NERC (ref. BB/M026620/01). The authors would like to thank the captains, crews, and fellow scientists from the many research vessels used to collect the samples utilized in this study. We thank Rhiannon Grant for assisting in preparing the samples for isotopic analysis and Tim Brand and Kirsty Black for assisting with the radiometric analysis of some of the samples at the Scottish Association of Marine Science. The authors thank Dr Bill Turrell (Marine Scotland) for comments on an early draft of the manuscript. Finally, the authors want to thank Sophie Hage, Sebastien Bertrand and Edward Anthony for insightful reviews that have improved the manuscript.

Author Contribution

WA and CS led the conception and design of the study. CS and WA carried out the fieldwork; CS undertook the laboratory research with support from HY (radiometric dating and interpolation). CS wrote the first draft of the manuscript; all authors contributed to the manuscript revision, and approved the submitted version.

References

Al-Qasmi, H., Law, G. T. W., Fifield, L. K., Howe, J. A., Brand, T., Cowie, G. L., … Livens, F. R. (2018). Deposition of artificial radionuclides in sediments of Loch Etive, Scotland. *Journal of Environmental Radioactivity*, *187*, 45–52.

Appleby, P.G., 2002. Chronostratigraphic techniques in recent sediments, in: Tracking Environmental Change Using Lake Sediments. Springer, pp. 171–203.

Appleby, P.G., Nolan, P.J., Gifford, D.W., Godfrey, M.J., Oldfield, F., Anderson, N.J., Battarbee, R.W., 1986. 210 Pb dating by low background gamma counting. Hydrobiologia 143, 21–27.

Appleby, P.G., Oldfield, F., 1992. Applications of lead-210 to sedimentation studies, in: Uranium-Series Disequilibrium: Applications to Earth, Marine, and Environmental Sciences. 2. Ed.

Appleby, P.G., Oldfield, F., 1978. The calculation of lead-210 dates assuming a constant rate of supply of unsupported 210Pb to the sediment. Catena 5, 1–8.

Aracena, C., Lange, C. B., Iriarte, J. L., Rebolledo, L., & Pantoja, S. (2011). Latitudinal patterns of export production recorded in surface sediments of the Chilean Patagonian fjords (41–55 S) as a response to water column productivity. *Continental Shelf Research*, *31*(3–4), 340–355.

Arias-Ortiz, A., Masqué, P., Garcia-Orellana, J., Serrano, O., Mazarrasa, I., Marbà, N., Lovelock, C.E., Lavery, P.S., Duarte, C.M., 2018. Reviews and syntheses: 210 Pb-derived sediment and carbon accumulation rates in vegetated coastal ecosystems–setting the record straight. Biogeosciences.

Arndt, S., Jørgensen, B.B., Larowe, D.E., Middelburg, J.J., Pancost, R.D., Regnier, P., 2013.

Earth-Science Reviews Quantifying the degradation of organic matter in marine sediments : A review and synthesis. Earth Sci. Rev. 123, 53–86. https://doi.org/10.1016/j.earscirev.2013.02.008

Austin, W.E.N., Inall, M.E., 2002. Deep-water renewal in a Scottish fjord : temperature , salinity and oxygen isotopes. Polar Res. 21, 251–257.

Avitabile, V., Herold, M., Heuvelink, G.B.M., Lewis, S.L., Phillips, O.L., Asner, G.P., Armston, J., Ashton, P.S., Banin, L., Bayol, N., 2016. An integrated pan-tropical biomass map using multiple reference datasets. Glob. Chang. Biol. 22, 1406–1420.

Avitabile, V., Herold, M., Lewis, S.L., Phillips, O.L., Aguilar-Amuchastegui, N., Asner, G.P., Brienen, R.J.W., DeVries, B.R., Gatti, R.G., Feldpausch, T.R., 2014. Comparative analysis and fusion for improved global biomass mapping, in: International Conference GV2M, Avignon, France. pp. 251–252.

Baskaran, M., Bianchi, T.S., Filley, T.R., 2017. Inconsistencies between 14C and short-lived radionuclides-based sediment accumulation rates: effects of long-term remineralization. J. Environ. Radioact. 174, 10–16.

Bertrand, S., Hughen, K.A., Sepulveda, J., Pantoja, S., 2012. Geochemistry of surface sediments from the fjords of Northern Chilean Patagonia (44–47 S): Spatial variability and implications for paleoclimate reconstructions. Geochim. Cosmochim. Acta 76, 125–146.

Bianchi, T.S., Arndt, S., Austin, W.E.N., Benn, D.I., Bertrand, S., Cui, X., Faust, J.C., Koziorowska-makuch, K., Moy, C.M., Savage, C., Smeaton, C., Smith, R.W., Syvitski, J., 2020. Earth-Science Reviews Fjords as Aquatic Critical Zones (ACZs). Earth-Science Rev. 203, 103145. https://doi.org/10.1016/j.earscirev.2020.103145

Bianchi, T.S., Galy, V., Rosenheim, B.E., Shields, M., Cui, X., Van Metre, P., 2015. Paleoreconstruction of organic carbon inputs to an oxbow lake in the Mississippi River watershed: Effects of dam construction and land use change on regional inputs. Geophys. Res. Lett. 42, 7983–7991.

Bird, M.I., Fifield, L.K., Chua, S., Goh, B., 2004. Calculating Sediment Compaction for Radiocarbon Dating of Intertidal Sediments. Radiocarbon 46, 421–435.

Blair, N.E., Aller, R.C., 2012. The Fate of Terrestrial Organic Carbon in the Marine Environment. Annaul Rev. Mar. Sci. 4, 401–423. https://doi.org/10.1146/annurev-marine-120709-142717

Bradwell, T., Fabel, D., Clark, C.D., Chiverrell, R.C., Small, D., Smedley, R.K., Saher, M.H., Moreton, S.G., Dove, D., Callard, S.L., 2021. Pattern, style and timing of British–Irish Ice Sheet advance and retreat over the last 45 000 years: evidence from NW Scotland and the adjacent continental shelf. J. Quat. Sci.

Bragg, O.M., Tallis, J.H., 2001. The sensitivity of peat-covered upland landscapes. Catena 42, 345–360.

Brown, F. S., Baedecker, M. J., Nissenbaum, A., & Kaplan, I. R. (1972). Early diagenesis in a reducing fjord, Saanich Inlet, British Columbia—III. Changes in organic constituents of sediment. *Geochimica et Cosmochimica Acta*, *36*(11), 1185–1203.

Burrows, M.T., Hughes, D.J., Austin, W.E.N., Smeaton, C., Hicks, N., Howe, J.A., Allen, C., Taylor, P., Vare, L.L., 2017. Assessment of blue carbon resources in Scotland's inshore marine protected area network. Scottish Nat. Herit. Comm. Rep. 957.

Burrows, M.T., Kamenos, N.A., Hughes, D.J., Stahl, H., Howe, J.A., Tett, P., 2014. Assessment of carbon budgets and potential blue carbon stores in Scotland's coastal and marine environment.

Cage, A. G., & Austin, W. E. N. (2010). Marine climate variability during the last millennium: The Loch Sunart record, Scotland, UK. *Quaternary Science Reviews*, *29*(13–14), 1633–1647.

Cage, A.G., Heinemeier, J., Austin, W.E.N., 2006. Marine radiocarbon reservoir ages in Scottish coastal and fjordic waters. Radiocarbon 48, 31–43.

Clark, C.D., Hughes, A.L.C., Greenwood, S.L., Jordan, C., Sejrup, H.P., 2012. Pattern and timing of retreat of the last British-Irish Ice Sheet. Quat. Sci. Rev. 44, 112–146.

Cui, X., Bianchi, T.S., Savage, C., Smith, R.W., 2016. Organic carbon burial in fjords : Terrestrial versus marine inputs. Earth Planet. Sci. Lett. 451, 41–50. https://doi.org/10.1016/j.epsl.2016.07.003

Dadey, K.A., Janecek, T., Klaus, A., 1992. Dry bulk density: its use and determination. Proc. Ocean Drill. Program, Sci. Results 126, 551–554.

Davies, J.M., 1975. Energy flow through the benthos in a Scottish sea loch. Mar. Biol. 31, 353–362.

Derrien, M., Choi, H., Jardé, E., Shin, K.-H., Hur, J., 2020. Do early diagenetic processes affect the applicability of commonly-used organic matter source tracking tools? An assessment through controlled degradation end-member mixing experiments. Water Res. 173, 115588.

Duffield, C. J., Alve, E., Andersen, N., Andersen, T. J., Hess, S., & Strohmeier, T. (2017). Spatial and temporal organic carbon burial along a fjord to coast transect : A case study from Western Norway. *Holocene*, *27*(9), 1325–1339. https://doi.org/10.1177/0959683617690588

Edwards, A., Sharples, F., 1986. Scottish sea lochs: a catalogue. Scottish Marine Biological Association.

Faust, J. C., Knies, J., Milzer, G., & Giraudeau, J. (2014). Terrigenous input to a fjord in central Norway records the environmental response to the North Atlantic Oscillation over the past 50 years. *The Holocene*, *24*(11), 1411–1418.

Faust, J.C., Knies, J., 2019. Organic Matter Sources in North Atlantic Fjord Sediments. Geochemistry, Geophys. Geosystems 20, 2872–2885. https://doi.org/10.1029/2019GC008382

Fernandes, R., Millard, A.R., Brabec, M., Marie-Josee, N., Grootes, P., 2014. Food Reconstruction Using Isotopic Transferred Signals (FRUITS): A Bayesian Model for Diet Reconstruction. PLoS One 9, 1–9. https://doi.org/10.1371/journal.pone.0087436

Folk, R.L., 1954. The distinction between grain size and mineral composition in sedimentary-rock nomenclature. J. Geol. 62, 344–359.

Friedrich, J., Janssen, F., Aleynik, D., Bange, H.W., Boltacheva, N.A., Çağatay, M.N., Dale, A.W., Etiope, G., Erdem, Z., Geraga, M., 2014. Investigating hypoxia in aquatic environments: diverse approaches to addressing a complex phenomenon. Biogeosciences 11, 1215–1259.

Gillibrand, P.A., Amundrud, T.L., 2007. A numerical study of the tidal circulation and buoyancy effects in a Scottish fjord : Loch Torridon. J. Geophys. Res. Ocean. 112, 1–22. https://doi.org/10.1029/2006JC003806

Gillibrand, P.A., Cage, A.G., Austin, W.E.N., 2005. A preliminary investigation of basin water response to climate forcing in a Scottish fjord : evaluating the influence of the NAO. Cont. Shelf Res. 25, 571–587. https://doi.org/10.1016/j.csr.2004.10.011

Gillibrand, P.A., Turrell, W.R., Moore, D.C., Adams, R.D., 1996. Bottom water stagnation and oxygen depletion in a Scottish sea loch. Estuar. Coast. Shelf Sci. 43, 217–235.

Glud, R.N., Berg, P., Stahl, H., Hume, A., Larsen, M., Eyre, B.D., Cook, P.L.M., 2016. Benthic carbon mineralization and nutrient turnover in a Scottish sea loch: an integrative in situ study. Aquat. geochemistry 22, 443–467.

Haas, H. De, Boer, W., Weering, T.C.E. Van, 1997. Recent sedimentation and organic carbon burial in a shelf sea : the North Sea. Mar. Geol. 144, 131–146.

Hage, S., Galy, V. V, Cartigny, M.J.B., Acikalin, S., Clare, M.A., Gröcke, D.R., Hilton, R.G., Hunt, J.E., Lintern, D.G., McGhee, C.A., 2020. Efficient preservation of young terrestrial organic carbon in sandy turbidity-current deposits. Geology 48, 882–887.

Harris, D., Horwa, W.R., Kessel, C. Van, 2001. Acid Fumigation of Soils to Remove Carbonates Prior to Total Organic Carbon or Carbon-13 Isotopic Analysis. Soil Sci. Soc. Am. J. 65, 1853–1856. https://doi.org/10.2136/sssaj2001.1853

Hayes, P., 2001. *Diagenetic processes and metal mobilisation in an organic rich Scottish fjord*. University of Leeds

Heath, M.R., Edwards, A.C., Patsch, J., Turrell, W.R., 2002. Modelling the behaviour of nutrients in the coastal waters of Scotland.

Heaton, Timothy J, Köhler, P., Butzin, M., Bard, E., Reimer, R.W., Austin, W.E.N., Ramsey, C.B., Grootes, P.M., Hughen, K.A., Kromer, B., Reimer, P.J., Heaton, T J, 2020. Marine20 — The marine radiocarbon age calibration curve (0-55,000 Cal BP). Radiocarbon 1–42. https://doi.org/10.1017/RDC.2020.68

Hemingway, J.D., Rothman, D.H., Grant, K.E., Rosengard, S.Z., Eglinton, T.I., Derry, L.A., Valier, V., 2019. Mineral protection regulates long-term global preservation of natural organic carbon. Nature 570. https://doi.org/10.1038/s41586-019-1280-6

Hinjosa, J.L., Moy, C.M., Stirling, C.H., Wilson, G.S., Eglinton, T.I., 2014. Carbon cycling and burial in New Zealand ' s fjords. Geochemistry, Geophys. Geosystems 4047–4063. https://doi.org/10.1002/2014GC005433.Received

Holt, J., Schrum, C., Cannaby, H., Daewel, U., Allen, I., Artioli, Y., Bopp, L., Butenschon, M., Fach, B.A., Harle, J., 2016. Potential impacts of climate change on the primary production of regional seas: A comparative analysis of five European seas. Prog. Oceanogr. 140, 91–115.

Howe, J.A., Austin, W.E.N., Forwick, M., Paetzel, M., Harland, R.E.X., Cage, A.G., 2010. Fjord systems and archives : a review. Fjord Syst. Arch. Geol. Soc. London, Spec. Publ. 5–15.

Howe, J.A., Shimmield, T., Austin, W.E.N., Longva, O., 2002. Post-glacial depositional environments in a mid-high latitude glacially-overdeepened sea loch , inner Loch Etive , western Scotland. Mar. Geol. 185, 417–433.

Huguet, C., Smittenberg, R. H., Boer, W., Damsté, J. S. S., & Schouten, S. (2007). Twentieth century proxy records of temperature and soil organic matter input in the Drammensfjord, southern Norway. *Organic Geochemistry*, *38*(11), 1838–1849.

Hunt, C.A., Demsar, U., Dayton, D., Smeaton, C., Cooper, R., Austin, W.E.N., 2020. Quantifying Marine Sedimentary Carbon: a new spatial analysis approach using seafloor acoustics, imagery, and ground-truthing data in Scotland. Front. Mar. Sci. https://doi.org/10.3389/fmars.2020.00588

Ingall, E., Kolowith, L., Lyons, T., & Hurtgen, M. (2005). Sediment carbon, nitrogen and phosphorus cycling in an anoxic fjord, Effingham Inlet, British Columbia. *American*

Journal of Science, *305*(3), 240–258.

Johnston, C.S., Jones, R.G., Hunt, R.D., 1977. A seasonal carbon budget for a laminarian population in a Scottish sea-loch. Helgoländer Wissenschaftliche Meeresuntersuchungen 30, 527–545.

Kaskela, A.M., Kotilainen, A.T., Alanen, U., Cooper, R., Green, S., Guinan, J., van Heteren, S., Kihlman, S., Van Lancker, V., Stevenson, A., 2019. Picking up the pieces—harmonising and collating seabed substrate data for European maritime areas. Geosciences 9, 84.

Keil, R.G., Mayer, L.M., 2014. Mineral matrices and organic matter.

Keil, R.G., Mayer, L.M., Quay, P.D., Richey, J.E., Hedges, J.I., 1997. Loss of organic matter from riverine particles in deltas. Geochim. Cosmochim. Acta 61, 1507–1511.

Kennedy, P., Kennedy, H., Papadimitriou, S., 2005. The effect of acidification on the determination of organic carbon , total nitrogen and their stable isotopic composition in algae and marine sediment. Rapid Commun. Mass Spectrom. 1063–1068. https://doi.org/10.1002/rcm.1889.

Knudson, K. P., Hendy, I. L., & Neil, H. L. (2011). Re-examining Southern Hemisphere westerly wind behavior: insights from a late Holocene precipitation reconstruction using New Zealand fjord sediments. *Quaternary Science Reviews*, *30*(21–22), 3124–3138.

Koziorowska, K., Kuli, K., Pempkowiak, J., 2018. ScienceDirect Comparison of the burial rate estimation methods of organic and inorganic carbon and quanti fi cation of carbon burial in two high Arctic fjords. Oceanologia 60, 405–418. https://doi.org/10.1016/j.oceano.2018.02.005

Krishnaswamy, S., Lal, D., Martin, J.M., Meybeck, M., 1971. Geochronology of lake sediments. Earth Planet. Sci. Lett. 11, 407–414.

Lalonde, K., Mucci, A., Ouellet, A., Ge, Y., 2012. Preservation of organic matter in sediments promoted by iron. Nature 483, 8–10. https://doi.org/10.1038/nature10855

Larowe, D.E., Arndt, S., Bradley, J.A., Estes, E.R., Hoarfrost, A., Lang, S.Q., Lloyd, K.G., Mahmoudi, N., Orsi, W.D., Walter, S.R.S., Steen, A.D., Zhao, R., 2020. Earth-Science Reviews The fate of organic carbon in marine sediments - New insights from recent data and analysis. Earth-Science Rev. 204, 103146. https://doi.org/10.1016/j.earscirev.2020.103146

Lee, H., Galy, V., Feng, X., Ponton, C., Galy, A., France-Lanord, C., Feakins, S.J., 2019. Sustained wood burial in the Bengal Fan over the last 19 My. Proc. Natl. Acad. Sci. 116, 22518–22525.

Leifeld, J., Steffens, M., Galego-Sala, A., 2012. Sensitivity of peatland carbon loss to organic matter quality. Geophys. Res. Lett. 39.

Li, D., Yao, P., Bianchi, T.S., Zhang, T., Zhao, B., Pan, H., Wang, J., Yu, Z., 2014. Organic carbon cycling in sediments of the Changjiang Estuary and adjacent shelf: Implication for the influence of Three Gorges Dam. J. Mar. Syst. 139, 409–419.

Louchouarn, P., Lucotte, M., Canuel, R., Gagne, J.-P., & Richard, L.-F. (1997). Sources and early diagenesis of lignin and bulk organic matter in the sediments of the Lower St. Lawrence Estuary and the Saguenay Fjord. *Marine Chemistry*, *58*(1–2), 3–26.

Loh, P.S., Reeves, A.D., Miller, A.E.J., Harvey, S.M., Overnell, J., 2010. Sediment fluxes and carbon budgets in Loch Creran, western Scotland. Geol. Soc. London, Spec. Publ. 344, 103–124.

Lunn, D., Spiegelhalter, D., Thomas, A., Best, N., 2009. The BUGS project: Evolution, critique and future directions. Stat. Med. 28, 3049–3067.

Malcolm, S. J. (1981). *Chemistry of sediments of Loch Etive, Scotland*. University of Edinburgh.

Mayer, L.M., 1994. Relationships between mineral surfaces and organic carbon concentrations in soils and sediments. Chem. Geol. 114, 347–363.

Mayr, C., Rebolledo, L., Schulte, K., Schuster, A., Zolitschka, B., Försterra, G., & Häussermann, V. (2014). Responses of nitrogen and carbon deposition rates in Comau Fjord (42 S, Southern Chile) to natural and anthropogenic impacts during the last century. *Continental Shelf Research*, *78*, 29–38.

McBreen, F., Wilson, J.G., Mackie, A.S.Y., Aonghusa, C.N., 2008. Seabed mapping in the southern Irish Sea: predicting benthic biological communities based on sediment characteristics, in: Challenges to Marine Ecosystems. Springer, pp. 93–103.

Middelburg, J.J., 2019. Carbon Processing at the Seafloor, in: Marine Carbon Biogeochemistry : A Primer for Earth System Scientists. Springer International Publishing, Cham, pp. 57–75. https://doi.org/10.1007/978-3-030-10822-9_4

Middelburg, J.J., 2018. Reviews and syntheses : to the bottom of carbon processing at the seafloor. Biogeosciences 15, 413–427.

Moffat, A.J., 1988. Forestry and soil erosion in Britain–a review. Soil Use Manag. 4, 41–44.

Moossen, H., Abell, R., Quillmann, U., Bendle, J., 2013. Holocene changes in marine productivity and terrestrial organic carbon inputs into an Icelandic fjord: Application of molecular and bulk organic proxies. The Holocene 23, 1699–1710.

Müller, A. (2001). Geochemical expressions of anoxic conditions in Nordåsvannet, a land-locked fjord in western Norway. *Applied Geochemistry*, *16*(3), 363–374.

Nordberg, K., Filipsson, H. L., Gustafsson, M., Harland, R., & Roos, P. (2001). Climate, hydrographic variations and marine benthic hypoxia in Koljö Fjord, Sweden. *Journal of Sea Research*, *46*(3–4), 187–200.

Nordberg, K., Filipsson, H. L., Linné, P., & Gustafsson, M. (2009). Stable oxygen and carbon isotope information on the establishment of a new, opportunistic foraminiferal fauna in a Swedish Skagerrak fjord basin, in 1979/1980. *Marine Micropaleontology*, *73*(1–2), 117–128.

Nørgaard-pedersen, N., Austin, W.E.N., Howe, J.A., Shimmield, T., 2006. The Holocene record of Loch Etive , western Scotland : Influence of catchment and relative sea level changes. Mar. Geol. 228, 55–71. https://doi.org/10.1016/j.margeo.2006.01.001

Nuwer, J. M., & Keil, R. G. (2005). Sedimentary organic matter geochemistry of Clayoquot Sound, Vancouver Island, British Columbia. *Limnology and Oceanography*, *50*(4), 1119–1128.

Overnell, J., Young, S., 1995. Sedimentation and carbon flux in a Scottish sea loch, Loch Linnhe. Estuar. Coast. Shelf Sci. 41, 361–376.

Pelegrí, J.L., Marrero-Díaz, A., Ratsimandresy, A.W., 2006. Nutrient irrigation of the North Atlantic. Prog. Oceanogr. 70, 366–406.

Perdue, E.M., Koprivnjak, J.-F., 2007. Using the C/N ratio to estimate terrigenous inputs of organic matter to aquatic environments. Estuar. Coast. Shelf Sci. 73, 65–72.

Prior, D.B., Bornhold, B.D., Johns, M.W., 1986. Active sand transport along a fjord-bottom channel, Bute Inlet, British Columbia. Geology 14, 581–584.

Ramirez, M.T., Allison, M.A., Bianchi, T.S., Cui, X., Savage, C., Schüller, S.E., Smith, R.W., Vetter, L., 2016. Modern deposition rates and patterns of organic carbon burial in

Fiordland, New Zealand. Geophys. Res. Lett. 43, 768–776. https://doi.org/10.1002/2016GL070021

Ramsey, C.B., Lee, S., 2013. Recent and planned developments of the program OxCal. Radiocarbon 55, 720–730.

Reimer, Paula J, Austin, W.E.N., Bard, E., Bayliss, A., Blackwell, P.G., Bronk, C., Butzin, M., Cheng, H., Edwards, R.L., Friedrich, M., Grootes, P.M., Guilderson, T.P., Hajdas, I., Heaton, T.J., Hogg, A.G., Hughen, K.A., Kromer, B., Manning, S.W., Muscheler, R., Palmer, J.G., Pearson, C., Plicht, J. Van Der, Reimer, R.W., Richards, D.A., Scott, E.M., Southon, J.R., Turney, C.S.M., Wacker, L., Adolphi, F., Reimer, P J, 2020. The Intcal20 Northern Hemisphere radiocarbon age calibration (0-55 Cal kBp). Rad 1–33. https://doi.org/10.1017/RDC.2020.41

Robbins, J.A., 1978. Geochemical and geophysical applications of radioactive lead. Biogeochem. Lead Environ. 285–393.

Sanchez-Cabeza, J.A., Ruiz-Fernández, A.C., 2012. 210Pb sediment radiochronology: an integrated formulation and classification of dating models. Geochim. Cosmochim. Acta 82, 183–200.

Santoro, M., Beaudoin, A., Beer, C., Cartus, O., Fransson, J.E.S., Hall, R.J., Pathe, C., Schmullius, C., Schepaschenko, D., Shvidenko, A., 2015. Forest growing stock volume of the northern hemisphere: Spatially explicit estimates for 2010 derived from Envisat ASAR. Remote Sens. Environ. 168, 316–334.

Sepulveda, J., Pantoja, A., Hughen, K., Lange, C., Gonzalez, F., Munoz, P., Rebolledo, L., Castro, R., Contrera, S., Avila, A., Rossel, P., Lorca, G., Salamanca, M., Silva, N., 2005. Fluctuations in export productivity over the last century from sediments of a southern Chilean fjord (44 S). Esturine Coast. Shelf Sci. 65, 587–600.

https://doi.org/10.1016/j.ecss.2005.07.005

Sepulveda, J., Pantoja, S., Hughen, K.A., 2011. Sources and distribution of organic matter in northern Patagonia fjords , Chile (44 – 47S): A multi-tracer approach for carbon cycling assessment. Cont. Shelf Res. 31, 315–329. https://doi.org/10.1016/j.csr.2010.05.013

Shepherd, C.J., Monroig, O., Tocher, D.R., 2017. Future availability of raw materials for salmon feeds and supply chain implications: The case of Scottish farmed salmon. Aquaculture 467, 49–62.

Shimmield, T. M. (1993). *A study of radionuclides, lead and lead isotope ratios in Scottish sea loch sediments*. University of Edinburgh.

Silva, N., Vargas, C. A., & Prego, R. (2011). Land–ocean distribution of allochthonous organic matter in surface sediments of the Chiloé and Aysén interior seas (Chilean Northern Patagonia). *Continental Shelf Research*, *31*(3–4), 330–339.

Simpson, J.H., Hill, A.E., 1986. The Scottish coastal current, in: The Role of Freshwater Outflow in Coastal Marine Ecosystems. Springer, pp. 295–308.

Smeaton, C., Austin, W.E.N., 2019. Where's the Carbon : Exploring the Spatial Heterogeneity of Sedimentary Carbon in Mid-Latitude Fjords. Front. Earth Sci. 7, 1–16. https://doi.org/10.3389/feart.2019.00269

Smeaton, C., Austin, W.E.N., 2017. Sources, Sinks, and Subsidies: Terrestrial Carbon Storage in Mid-latitude Fjords. J. Geophys. Res. Biogeosciences 122, 2754–2768. https://doi.org/10.1002/2017JG003952

Smeaton, C., Austin, W.E.N., Davies, A.L., Baltzer, A., Abell, R.E., Howe, J.A., 2016. Substantial stores of sedimentary carbon held in mid-latitude fjords. Biogeosciences

5771–5787. https://doi.org/10.5194/bg-13-5771-2016

Smeaton, C., Austin, W.E.N., Davies, A.L., Baltzer, A., Howe, J.A., Baxter, J.M., 2017. Scotland’s forgotten carbon : a national assessment of mid-latitude fjord sedimentary carbon stocks. Biogeosciences 14, 5663–5674.

Smeaton, C., Cui, X., Bianchi, T.S., Cage, A.G., Howe, J.A., Austin, W.E.N., 2021a. The evolution of a coastal carbon store over the last millennium. Quat. Sci. Rev. 266, 107081.

Smeaton, C., Hunt, C.A., Turrell, W.R., Austin, W.E.N., 2021b. Marine Sedimentary Carbon Stocks of the United Kingdom’s Exclusive Economic Zone. Front. Earth Sci. 9. https://doi.org/10.3389/feart.2021.593324

Smith, R.W., Bianchi, T.S., Allison, M., Savage, C., Galy, V., 2015. High rates of organic carbon burial in fjord sediments globally. Nat. Geosci. 8, 450–453. https://doi.org/10.1038/NGEO2421

Smith, R. W., Bianchi, T. S., & Savage, C. (2010). Comparison of lignin phenols and branched/isoprenoid tetraethers (BIT index) as indices of terrestrial organic matter in Doubtful Sound, Fiordland, New Zealand. *Organic Geochemistry*, *41*(3), 281–290. https://doi.org/10.1016/j.orggeochem.2009.10.009

Smittenberg, R H, Pancost, R. D., Hopmans, E. C., Paetzel, M., & Damsté, J. S. S. (2004). A 400-year record of environmental change in an euxinic fjord as revealed by the sedimentary biomarker record. *Palaeogeography, Palaeoclimatology, Palaeoecology*, *202*(3–4), 331–351.

Smittenberg, Rienk H, Baas, M., Green, M. J., Hopmans, E. C., Schouten, S., & Damsté, J. S. S. (2005). Pre-and post-industrial environmental changes as revealed by the biogeochemical sedimentary record of Drammensfjord, Norway. *Marine Geology*, *214*(1–3), 177–200.

Smout, T.C., 2004. History of the native woodlands of Scotland 1500-1920. Edinburgh University Press.

Smout, T.C., 2003. People and woods in Scotland. Edinburgh University Press.

Sparkes, R.B., Lin, I.-T., Hovius, N., Galy, A., Liu, J.T., Xu, X., Yang, R., 2015. Redistribution of multi-phase particulate organic carbon in a marine shelf and canyon system during an exceptional river flood: Effects of Typhoon Morakot on the Gaoping River–Canyon system. Mar. Geol. 363, 191–201.

Steele, J.H.T., Baird, I.E., 1962. Further relations between primary production, chlorophyll, and particulate carbon. Limnol. Oceanogr. 7, 42–47.

St-Onge, G., & Hillaire-Marcel, C. (2001). Isotopic constraints of sedimentary inputs and organic carbon burial rates in the Saguenay Fjord, Quebec. *Marine Geology*, *176*(1–4), 1–22.

Syvitski, J.P.M., Burrell, D.C., Skei, J.M., 1987. Fjords: processes and products. Springer Science & Business Media.

Syvitski, J.P.M., Shaw, J., 1995. Sedimentology and geomorphology of fjords, in: Developments in Sedimentology. Elsevier, pp. 113–178.

Tipping, R., 2014. Towards an Environmental History of Argyll & Bute: A Review of Current Data, Their Strengths and Weaknesses and Suggestions for Future Work.

Velinsky, D. J., & Fogel, M. L. (1999). Cycling of dissolved and particulate nitrogen and carbon in the Framvaren Fjord, Norway: stable isotopic variations. *Marine Chemistry*, *67*(3–4), 161–180.

Walsh, E. M., Ingalls, A. E., & Keil, R. G. (2008). Sources and transport of terrestrial organic matter in Vancouver Island fjords and the Vancouver-Washington Margin: A multiproxy approach using d13Corg, lignin phenols, and the ether lipid BIT index. *Limnology and Oceanography*, *53*(3), 1054–1063.

Watts, L.J., Rippeth, T.P., Edwards, A., 1998. The roles of hydrographic and biogeochemical processes in the distribution of dissolved inorganic nutrients in a Scottish sea-loch: consequences for the spring phytoplankton bloom. Estuar. Coast. Shelf Sci. 46, 39–50.

Włodarska-Kowalczuk, M., Mazurkiewicz, M., Górska, B., Michel, L.N., Jankowska, E., Zaborska, A., 2019. Organic carbon origin, benthic faunal consumption, and burial in sediments of Northern Atlantic and Arctic Fjords (60–81 N). J. Geophys. Res. Biogeosciences 124, 3737–3751.

Wood, B.J.B., Tett, P.B., Edwards, A., 1973. An introduction to the phytoplankton, primary production and relevant hydrography of Loch Etive. J. Ecol. 569–585.

Young, S.A., 1996. *Radionuclide tracer study of heavy metal cycling in Loch Etive, Scotland*. University of Edinburgh.

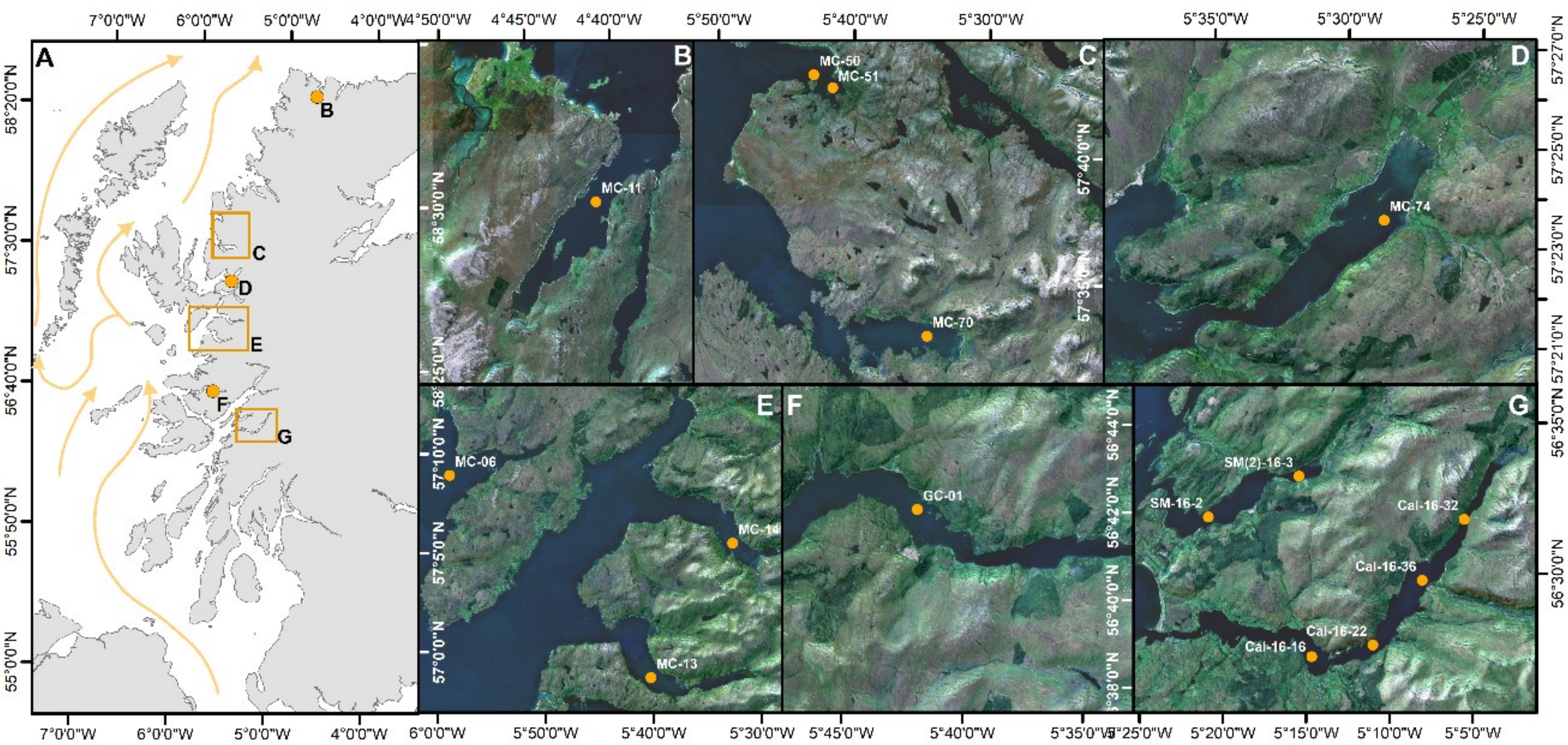

Figure 1. Locations of the fjords and associated coring sites investigated within this study. **(A)** Overview of **s**tudy sites with the Scottish Coastal Current (Simpson & Hill, 1986) the dominant current in the region represent by orange arrows. Coring sites at (**B**) Loch Eriboll (MC-11), (**C**) Loch Gairloch (MC50 and MC-51), (**D**) Loch Torridon (MC-74), (**E**) Loch Eishort (MC-06), Loch Nevis (MC-13 and Loch Hourn (MC-14), (**F**) Loch Sunart (GC-01) and (**G**) Loch Creran (SM-16-2, SM(2)-16-3) and Loch Etive (Cal-16-16, Cal-16-22, Cal-16-36, Cal-16-32). Further details of the coring sites can be found in supplementary table 1.

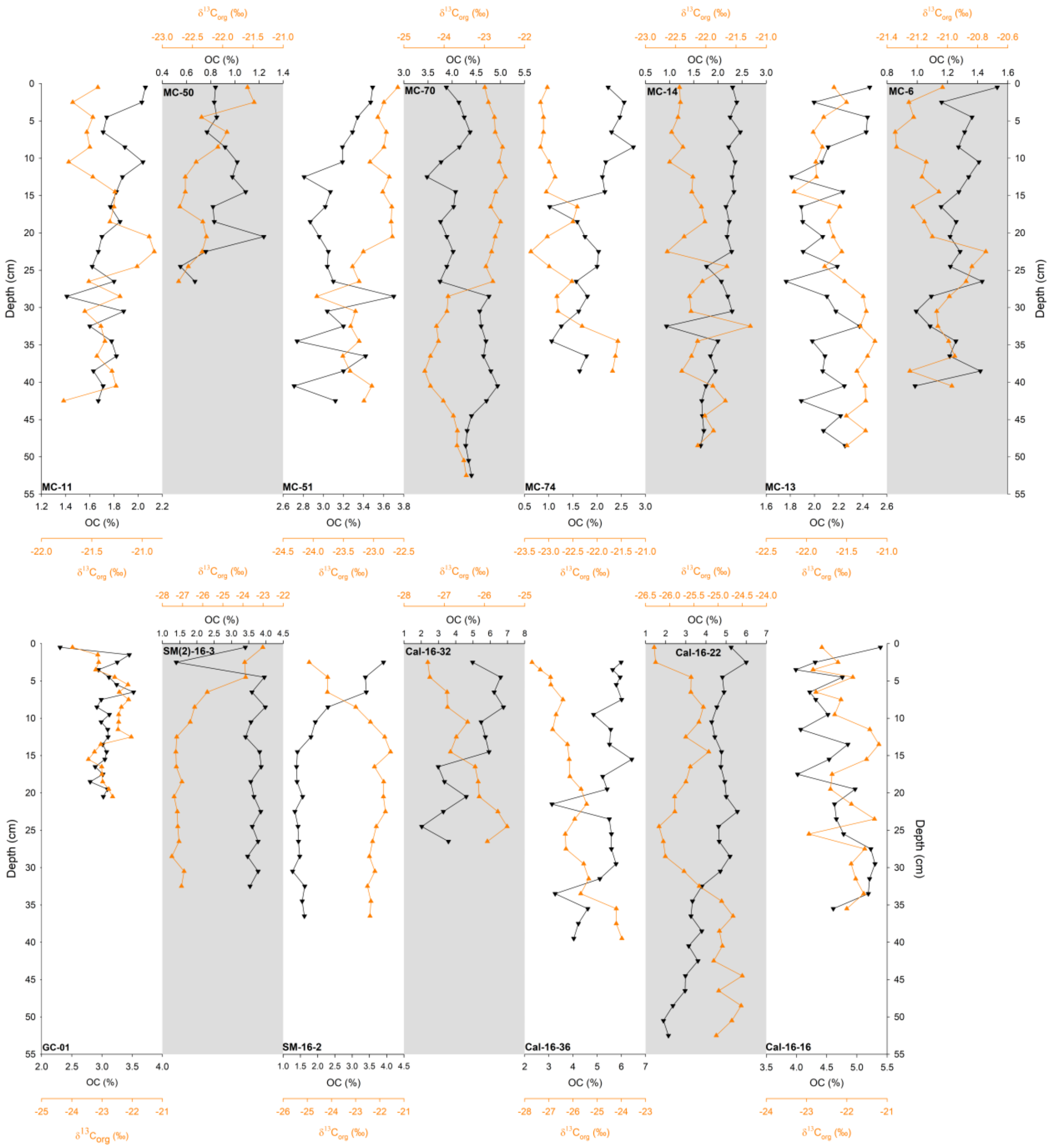

Figure 2. Down core OC (%) and $\delta^{13}C_{org}$ (‰) records for the fifteen sediment cores analysed as part of this project.

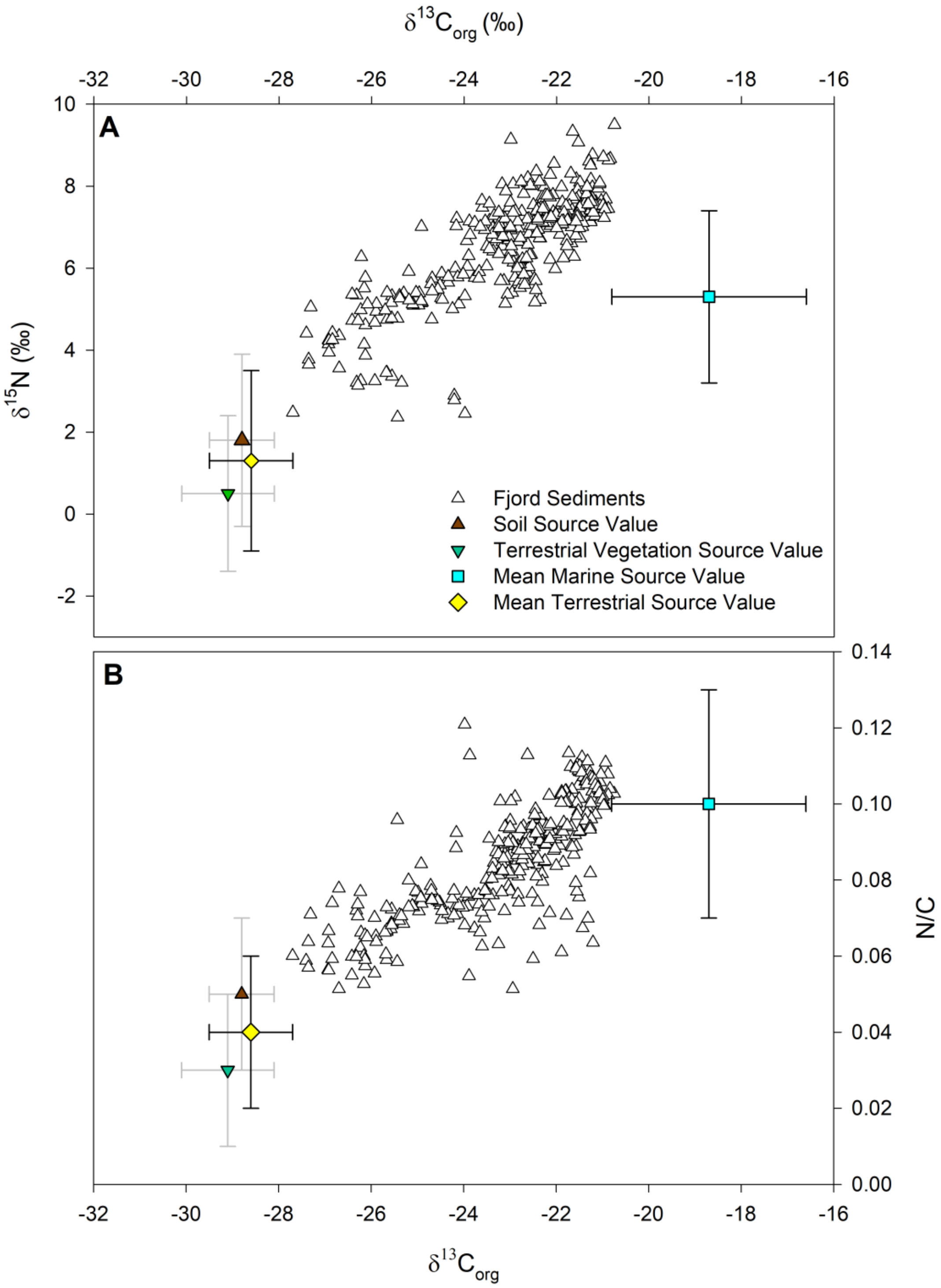

Figure 3. Cross plots (**A**) $\delta^{13}C_{org}$ versus $\delta^{15}N$ and (**B**) $\delta^{13}C_{org}$ versus N/C in surface sediment of ten Scottish fjords; shaded envelopes illustrate the range of the terrestrial and marine source values (*Supplementary Table 2-3*).

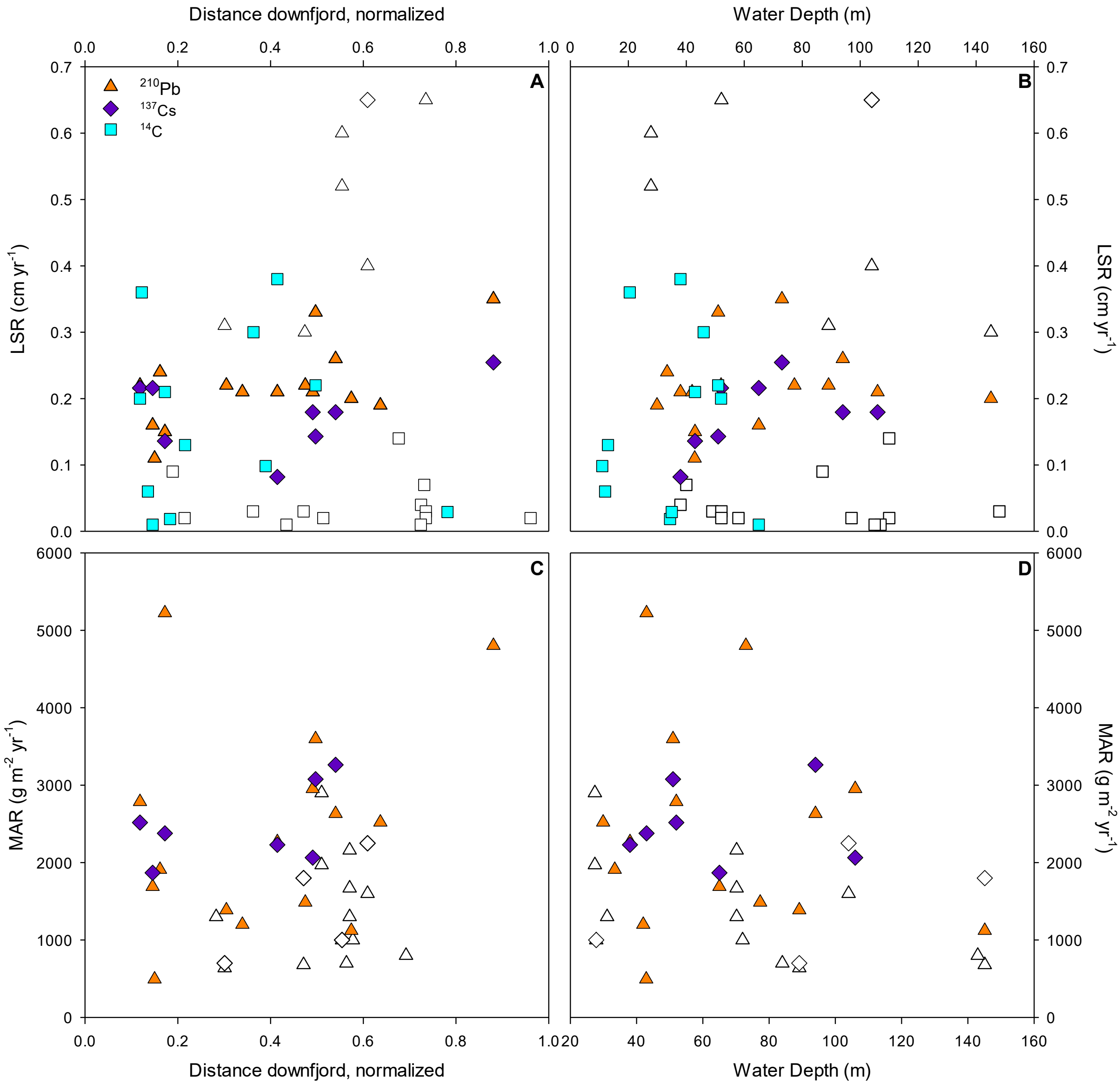

Figure 4. Differences in LSR and MAR calculated using different radiometric dating techniques. (**A**) LSR versus normalized distance down-fjord, (**B**) LSR versus water depth, (**C**) MAR versus normalized distance down-fjord, and (**D**) MAR versus water depth. Coloured symbols represent the calculated rates from this study, open symbols represent rates from the literature. Full dataset can be found in supplementary material.

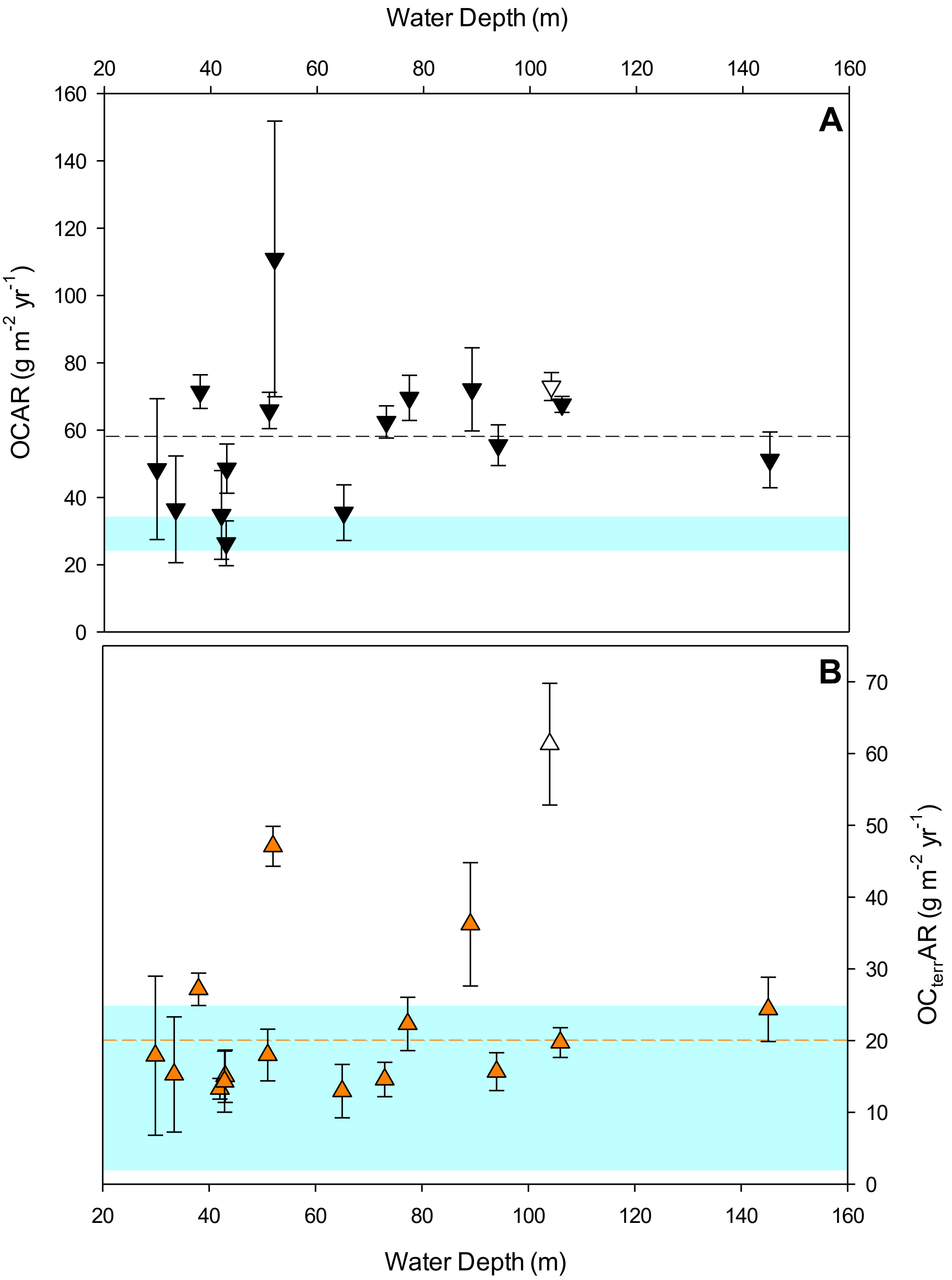

Figure 5. (**A**) OCAR versus water depth (m), (**B**) $OC_{terr}AR$ versus water depth (m). Shaded symbols are cores from this study; the open symbol represents data from Hayes (2001). The dotted lines represent the mean OCAR and $OC_{terr}AR$ for all the cores analysed in this study, the blue shading represents the range of mean values from other temperate vegetated fjords (Cui et al., 2016).

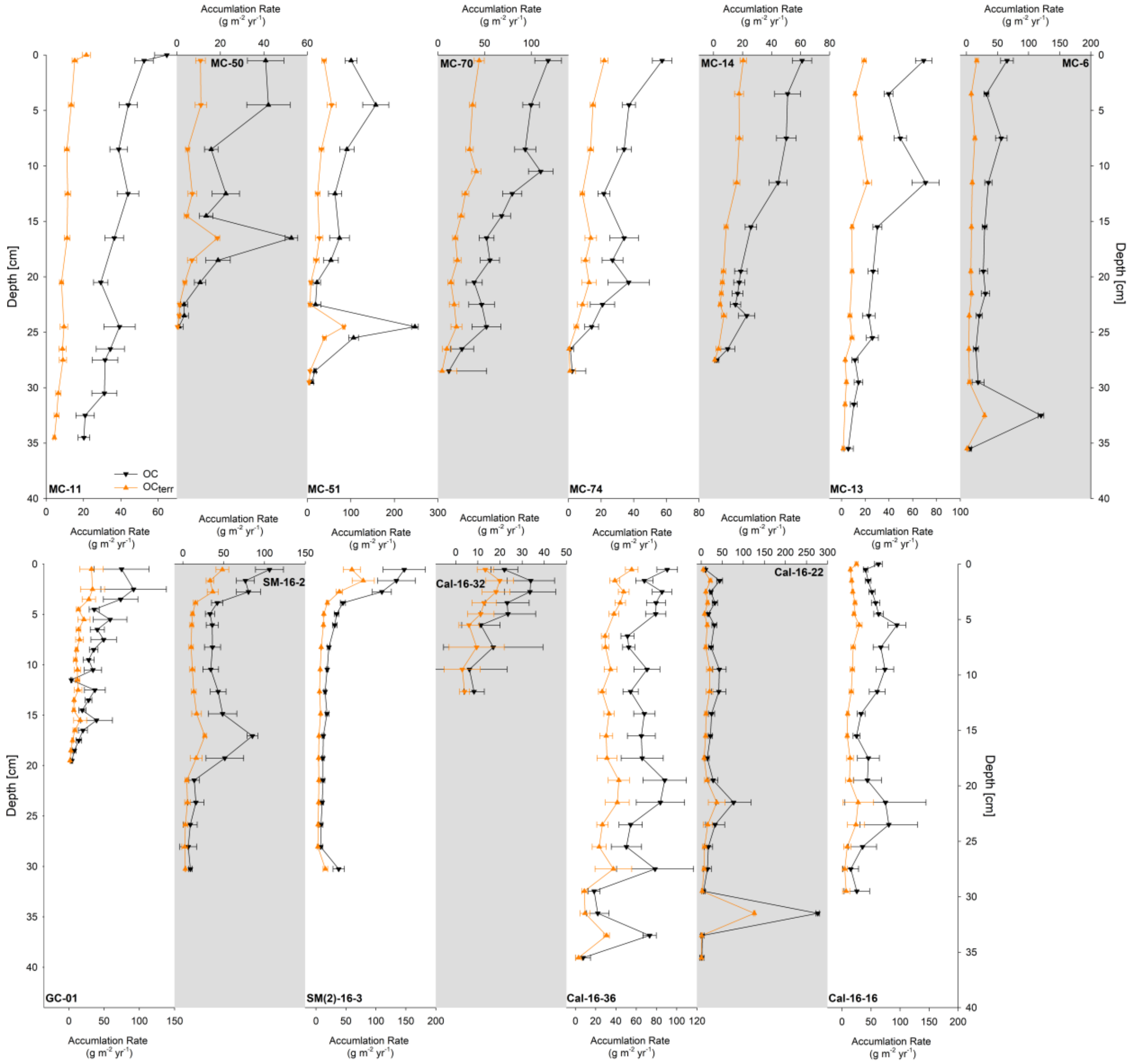

Figure 6. Down core OCAR (g m^{-2} yr^{-1}) and OC_{terr}AR (g m^{-2} yr^{-1}) records for the fifteen sediment cores collected from Scottish fjords as part of this study.

Core	Fjord	Mean (µm)	% < 63µm	Folk Class
MC-11	Eriboll	25.65 ± 6.86	86.87 ± 8.76	Mud to Muddy Sand
MC-50	Gairloch	62.94 ± 12.58	48.65 ± 17.65	Mixed
MC-51	Gairloch	28.62 ± 4.04	87.64 ± 3.56	Mud to Muddy Sand
MC-70	Torridon	21.27 ± 4.96	92.90 ± 3.98	Mud to Muddy Sand
MC-74	Carron	49.06 ± 12.66	66.18 ± 8.85	Mud to Muddy Sand
MC-14	Hourn	28.40 ± 11.67	84.03 ± 6.92	Mud to Muddy Sand
MC-13	Nevis	12.74 ± 2.12	98.51 ± 0.97	Mud to Muddy Sand
MC-06	Eishort	18.42 ± 3.04	94.27 ± 2.29	Mud to Muddy Sand
GC-01	Sunart	27.62 ± 6.07	91.77 ± 1.48	Mud to Muddy Sand
SM-16-2	Creran	53.50 ± 5.24	62.31 ± 4.76	Mud to Muddy Sand
SM(2)-16-3	Creran	22.57 ± 3.28	92.59 ± 2.12	Mud to Muddy Sand
Cal-16-32	Etive	27.61 ± 5.16	88.20 ± 3.53	Mud to Muddy Sand
Cal-16-36	Etive	31.54 ± 8.31	86.22 ± 6.20	Mud to Muddy Sand
Cal-16-22	Etive	41.59 ± 11.56	77.16 ± 6.74	Mud to Muddy Sand
Cal-16-16	Etive	36.10 ± 4.74	82.76 ± 3.74	Mud to Muddy Sand

Table 1. Grain size characteristics of each of the fifteen sediment cores. Mean (µm) and % <63 µm data calculated from all one cm slices of each core. The modified Folk classification scheme (Kaskela et al., 2019) was used to describe the sediment type. Full grain size data can be found in the supplementary data.

Core ID	Fjord	^{210}Pb LSR (cm yr^{-1})	^{137}Cs LSR (cm yr^{-1})	^{14}C LSR (cm yr^{-1})	^{210}Pb MAR (g m^{-2} yr^{-1})	^{137}Cs MAR (g m^{-2} yr^{-1})	Reference
MC-11	Loch Eriboll	0.33 ± 0.08	0.13 – 0.15	0.22 ± 0.05	3,598	1,937	
MC-50	Loch Gairloch	0.15 ± 0.06	0.13 – 0.15	0.21 ± 0.03	5,224	3,077	
MC-51	Loch Gairloch	0.21 ± 0.02	0.07 – 0.09	0.38 ± 0.11	2,268	2,378	
MC-70	Loch Torridon	0.22 ± 0.03	0.21 – 0.23	0.20 ± 0.01	2,786	2,229	
MC74	Loch Carron	0.16 ± 0.06	0.22 – 0.26	0.01 ± 0.01	1,689	2,517	
MC-14	Loch Hourn	0.21 ± 0.03	0.17 – 0.19		2,954	1,868	
MC-13	Loch Nevis	0.26 ± 0.04	0.16 – 0.19		2,632	2,064	
MC-6	Loch Eishort/Slapin	0.35 ± 0.04	0.25 – 0.26		4,803	3,263	*This Study*
GC-01	Loch Sunart	0.21 ± 0.02			1,200		
SM-16-2	Loch Creran	0.19 ± 0.1		0.26 ± 0.02	2,521		
SM(2)-16-3	Loch Creran	0.24 ± 0.02			1,910		
Cal-16-32	Loch Etive	0.11 ± 0.01			494		
Cal-16-36	Loch Etive	0.22 ± 0.07			1,387		
Cal-16-22	Loch Etive	0.20 ± 0.1			1,122		
Cal-16-16	Loch Etive	0.22 ± 0.04			1,487		
Other Scottish Fjords							
LD 1	Loch Duich	0.4	0.56 – 0.74		1,600	2,000-2,500	*Hayes, 2001*
PM06-MC-01	Loch Sunart	0.65 ± 0.41		0.56 ± 0.02			*Cage and Austin, 2010**
Upper Basin (RE 6)	Loch Etive	0.6					*Al-Qasmi et al., 2018*
Lower Basin (RE 5)	Loch Etive	0.3					
Upper Basin (RE 3)	Loch Etive	0.31					*Malcolm, 1981*
Lower Basin (RE 5)	Loch Etive	0.52					
LE1	Loch Etive				640	700	*Shimmield, 1993*
LE2	Loch Etive				680	1,800	
LE3	Loch Etive				1,000	1,000	
LL1	Long (Clyde)				1,000		
GD2	Loch Goil				700		
FS	Loch Fyne				800		
YA	Loch Etive				1,970		*Young, 1996*
YB	Loch Etive				1,670		
YC	Loch Etive				2,160		
LES-1	Loch Etive				1,300		*Ridgway, 1984*
LES-2	Loch Etive				2,900		
LES-3	Loch Etive				1,300		
Other Vegetated Temperate Fjords							
Norway		0.3 – 0.78			42.6 – 3319		*Duffield et al., 2017; Faust and Knies, 2019; Müller, 2001*
Patagonia (Chile)		0.14 – 0.47			897 – 2841		*Sepulveda et al., 2011*
New Zealand		0.06 – 0.38			51 – 2050		*Cui et al., 2016; Ramirez et al., 2016; Smith et al., 2015*

Table 2. LSR and MAR for the fifteen cores analysed in this study calculated using different radiometric dating techniques (^{210}Pb, ^{137}Cs, ^{14}C). Additionally, compiled rates from Scottish and other vegetated temperate fjords found in the literature are presented. * Radiocarbon data recalibrated using the Marine 20 calibration curve (Heaton et al., 2020)

Fjord	LSR (cm yr^{-1})	MAR (g m^{-2} yr^{-1})	OC (%)	OC_{terr} (%)	OCAR (gC m^{-2} yr^{-1})	$OC_{terr}AR$ (gC m^{-2} yr^{-1})	Reference
Loch Eriboll	0.33 ± 0.08	3598	1.8 ± 0.2	27.7	65.8 ± 5.4	18.0 ± 3.6	
Loch Gairloch	0.18 ± 0.04	3746 ± 2090	2.0 ± 0.2	36.1	60.0 ± 6.2	21.1 ± 3.0	
Loch Torridon	0.22 ± 0.03	2786	4.0 ± 1.5	39.5	110.9 ± 41.0	47.1 ± 2.8	
Loch Carron	0.16 ± 0.06	1689	2.1 ± 0.5	36.5	35.5 ± 8.3	12.9 ± 3.7	
Loch Hourn	0.21 ± 0.03	2954	2.3 ± 0.1	32.3	67.7 ± 2.4	19.7 ± 2.1	*This Study*
Loch Nevis	0.26 ± 0.04	2632	2.1 ± 0.2	28.1	55.5 ± 6.1	15.7 ± 2.6	
Loch Eishort/Slapin	0.35 ± 0.04	4803	1.3 ± 0.1	24.3	62.4 ± 4.8	14.6 ± 2.4	
Loch Sunart	0.21 ± 0.02	1200	3.0 ± 1.1	36.5	34.8 ± 13.2	13.3 ± 1.4	
Loch Creran	0.22 ± 0.06	2215 ± 432	1.9 ± 0.8	38.0	42.4 ± 18.4	16.6 ± 9.6	
Loch Etive	0.18 ± 0.06	1123 ± 446	4.9 ± 0.9	44.8	51.2 ± 8.5	24.3 ± 5.3	
Loch Duich	0.4	1600	4.7 ± 0.6	84.0	72.9 ± 4.2	61.3 ± 8.5	*Hayes, 2001*
Scottish Fjords	**0.25 ± 0.1**	**2577 ± 1159**	**2.74 ± 1.2**	**38.8**	**57.1 ± 10.9**	**20.9 ± 4.3**	
Other Vegetated Fjord Systems							
Patagonia	0.31	1270 ± 600	1.9 ± 0.8	42.3	24.0 ± 16.3	10.2 ± 10.7	(Aracena et al., 2011; Mayr et al., 2014; Sepúlveda et al., 2005; Silva et al., 2011)
West Canada	0.30	1750 ± 1870	1.6 ± 3.6	47.5	28.0 ± 3.1	13.3 ± 4	(Brown et al., 1972; Ingall et al., 2005; Nuwer and Keil, 2005; Smittenberg et al., 2004; Walsh et al., 2008)
East Canada	0.70	4770 ± 5440	0.7 ± 0.9	70.1	34.8 ± 71.6	24.4 ± 73.8	(Louchouarn et al., 1997; St-Onge and Hillaire-Marcel, 2001; Syvitski et al., 1987)
NW Europe	0.35	700 ± 710	4.2 ± 4.2	76.5	29.3 ± 17.3	14.3 ± 8.6	(Faust et al., 2014; Faust and Knies, 2019; Huguet et al., 2007; Loh et al., 2010; Müller, 2001; Nordberg et al., 2009, 2001; Smittenberg et al., 2005; Velinsky and Fogel, 1999)
New Zealand	0.14	880 ± 320	3.8 ± 1.9	73.4	33.8 ± 23.0	24.8 ± 20.9	(Cui et al., 2016; Knudson et al., 2011; Ramirez et al., 2016; Smith et al., 2015, 2010)

Table 3. OCAR and $OC_{terr}AR$ data for 10 mid-latitude fjords from Scotland. Mean values are presented for fjords with multiple cores (Loch Creran, Etive and Gairloch). Data from other vegetated fjord systems are included for comparison.

			All Sediments	Muddy Sediments	
Fjords	**Area** (km^2)	**Burial Efficiency** (%)	**OC Burial** (Tonnes yr^{-1})	**Mud** (%)	**OC Burial** (Tonnes yr^{-1})
Loch Eriboll	31.1	78.6	1,610 ± 132	51	819 ± 67
Loch Gairloch	13.8	92.8	769 ± 79	51	463 ± 32
Loch Torridon	70.0	94.0	7,293 ± 2,694	34	2,464 ± 910
Loch Carron	23.1	71.3	584 ± 136	43	254 ± 60
Loch Hourn	33.7	95.1	2,167 ± 76	49	1,070 ± 37
Loch Nevis	28.7	77.5	1,234 ± 135	28	342 ± 37
Loch Eishort/Slapin	45.6	85.0	2,419 ± 186	29	711 ± 55
Loch Sunart	49.5	81.2	1,398 ± 530	27	378 ± 143
Loch Creran	13.3	36.3	205 ± 89	27	55 ± 24
Loch Etive	29.5	75.2	1,134 ± 189	58	655 ± 109
Loch Duich	44.2	87.0	2,808 ± 161	27	760 ± 43

Table 4. Annual OC burial in the mid-latitude fjords of Scotland. Broken down into rates for the fjords as a whole and the muddy sediments alone. Supplementary figures 36-37 illustrate the spatial distribution of the different sediment types within the fjords.

	Area (km^2)	OCAR ($g\ m^{-2}\ yr^{-1}$)	Burial Efficiency (%)	OC Burial ($Mt\ yr^{-1}$)
Rock & Boulders	220.92	0	0	0
Coarse Sediment	505.70	—	—	—
Mixed Sediment	729.18	48.6 ± 7.3	88.0	0.038
Mud to muddy Sand	1,011.27	59.1 ± 22.1	76.4 (34.7 – 97.6)	0.046 (0.02 – 0.06)
Sand	141.24	—	—	—
Total	**2,608.31**			**0.084 (0.06 – 0.10)**

Table 5. National estimates of the total annual burial of OC within the different sediments of Scotland's fjords. Bracketed figures represent the min and max values. Data for coarse sediments and sand are not included and the total OC burial estimates are therefore underestimated. Areal extent of the different sediment types obtained from Smeaton et al. (2021) and Smeaton and Austin, (2019).